This journal is © The Partner Organisations 2014

Electronic Supplementary Information

Triptycene-derived calix[6]arene analogues: synthesis, structure and complexation with paraquat derivatives

Yu-Xiang Xia,[a,b] Tao Xie,[a] Ying Han[a] and Chuan-Feng Chen[a,*]

[a]*Beijing National Laboratory for Molecular Sciences, CAS Key laboratory of Molecular Recognition and Function, Institute of Chemistry, Chinese Academy of Sciences, Beijing 100190, China.* [b]*University of Chinese Academy of Sciences, Beijing 100049, China.*

E-mail: cchen@iccas.ac.cn

Contents

1. Copies of ^{1}H NMR and ^{13}C NMR spectra of new compounds

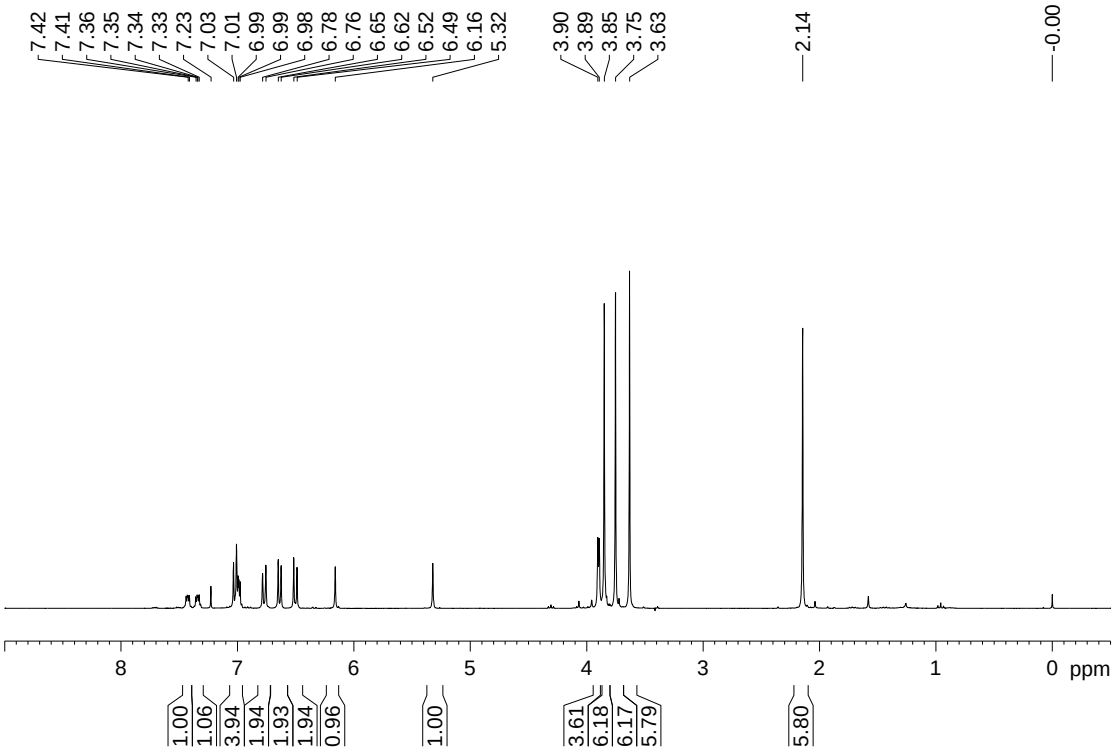

Fig. S1 ^{1}H NMR spectrum (300 MHz, $CDCl_3$) of **5**.

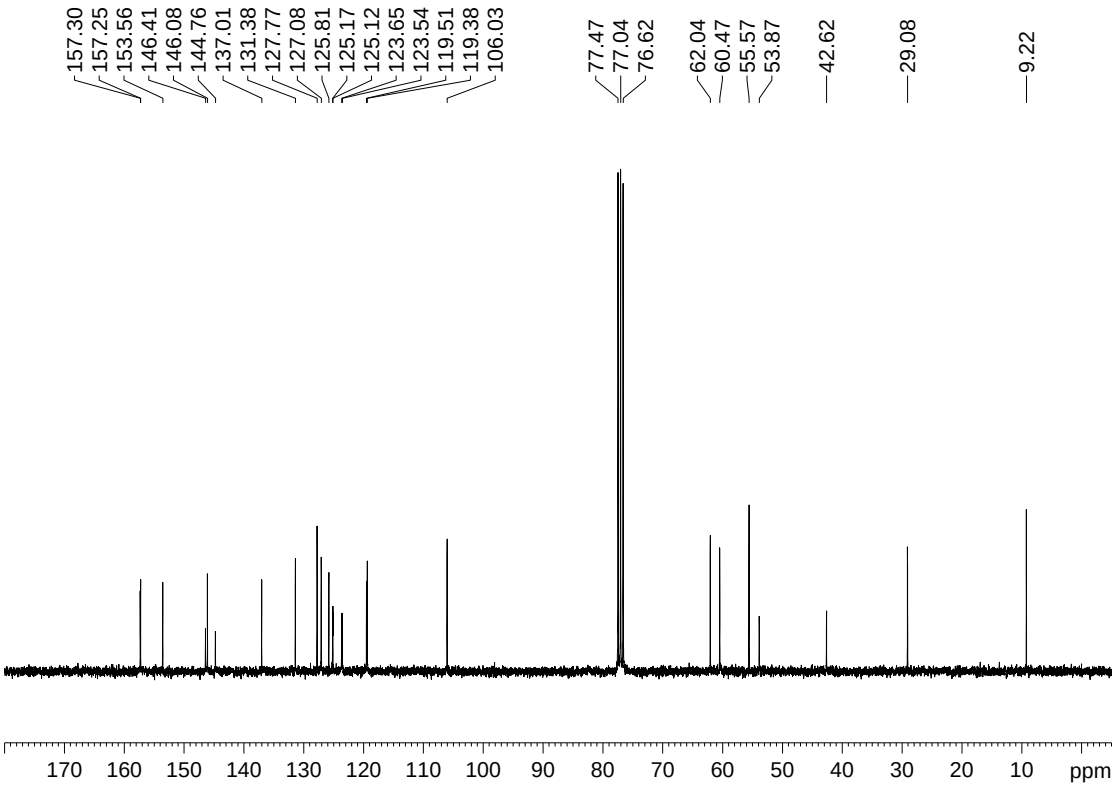

Fig. S2 ^{13}C NMR spectrum (75 MHz, $CDCl_3$) of **5**.

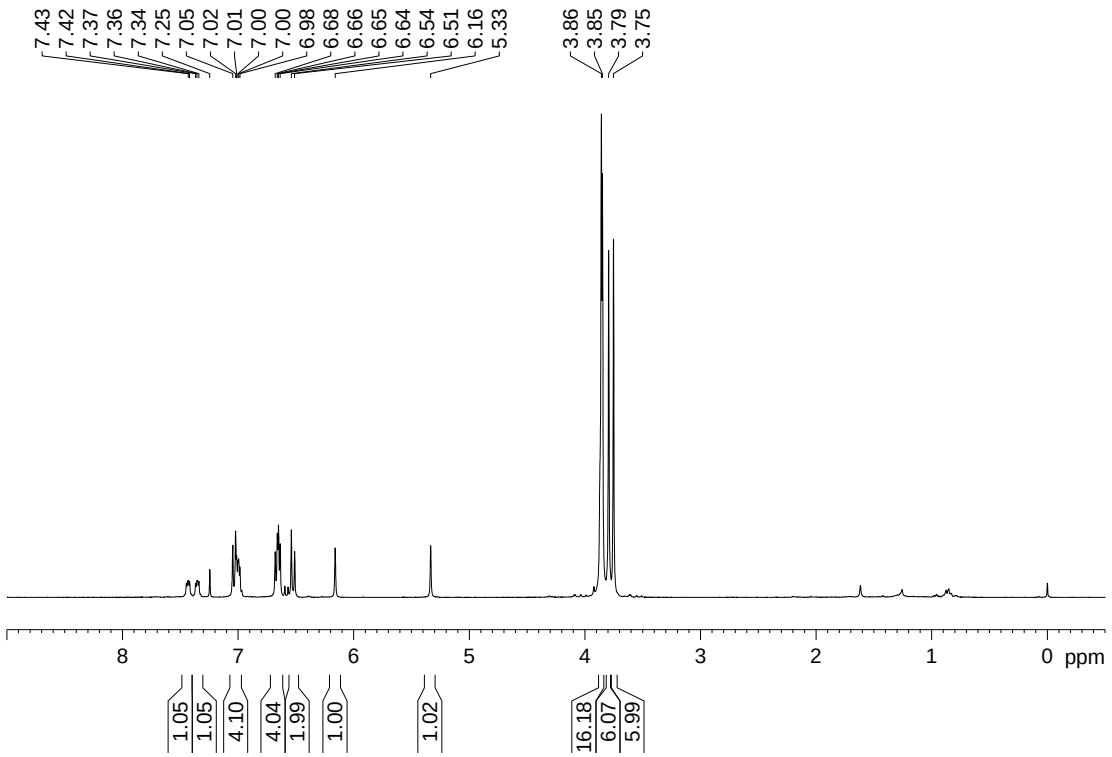

Fig. S3 ^{1}H NMR spectrum (300 MHz, $CDCl_3$) of **6**.

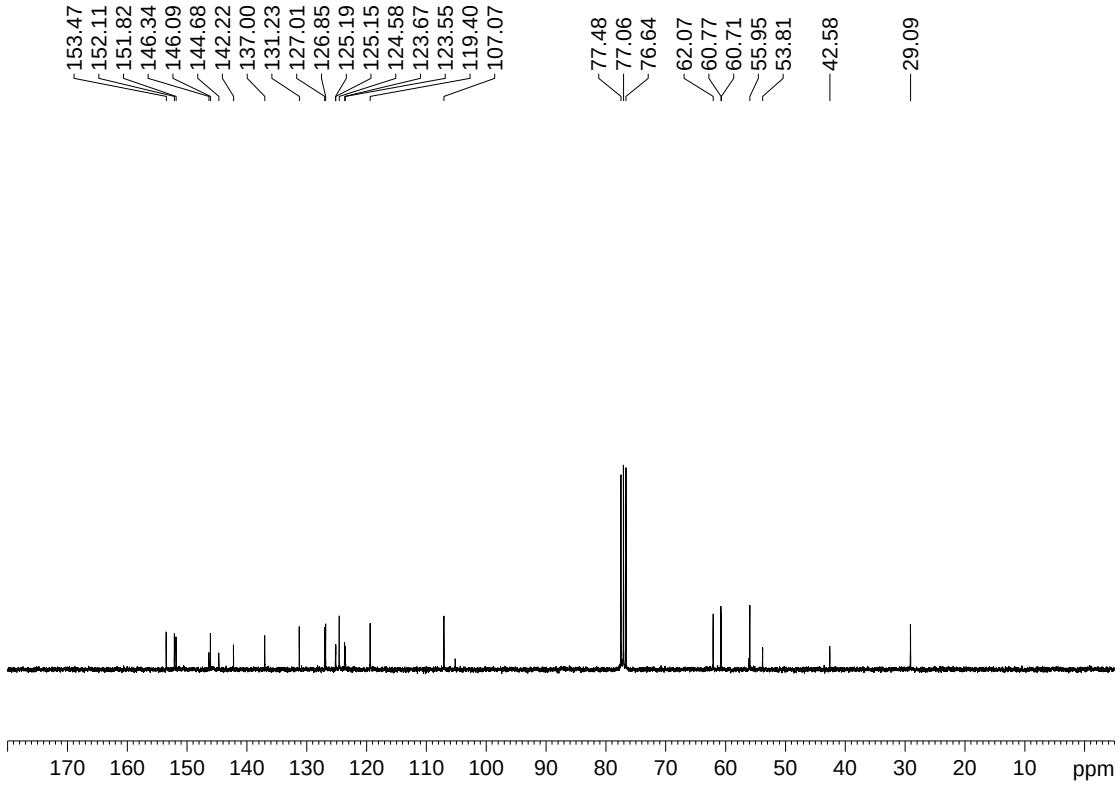

Fig. S4 ^{13}C NMR spectrum (75 MHz, $CDCl_3$) of **6**.

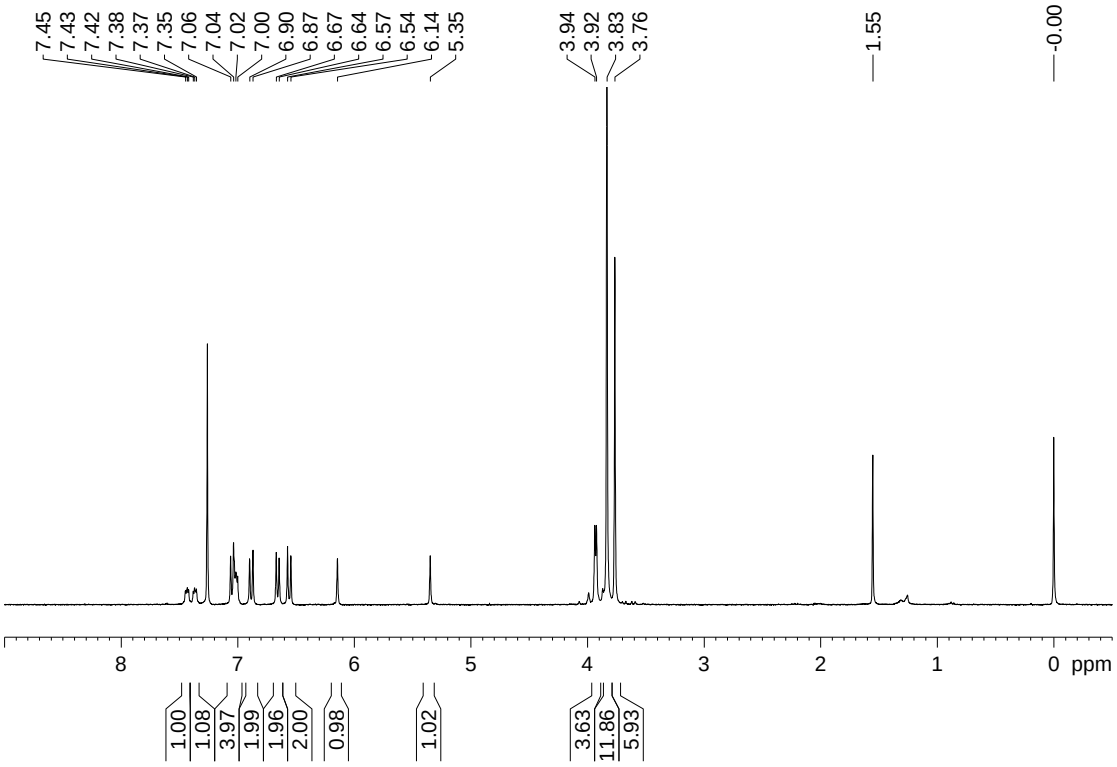

Fig. S5 ^{1}H NMR spectrum (300 MHz, $CDCl_3$) of **7**.

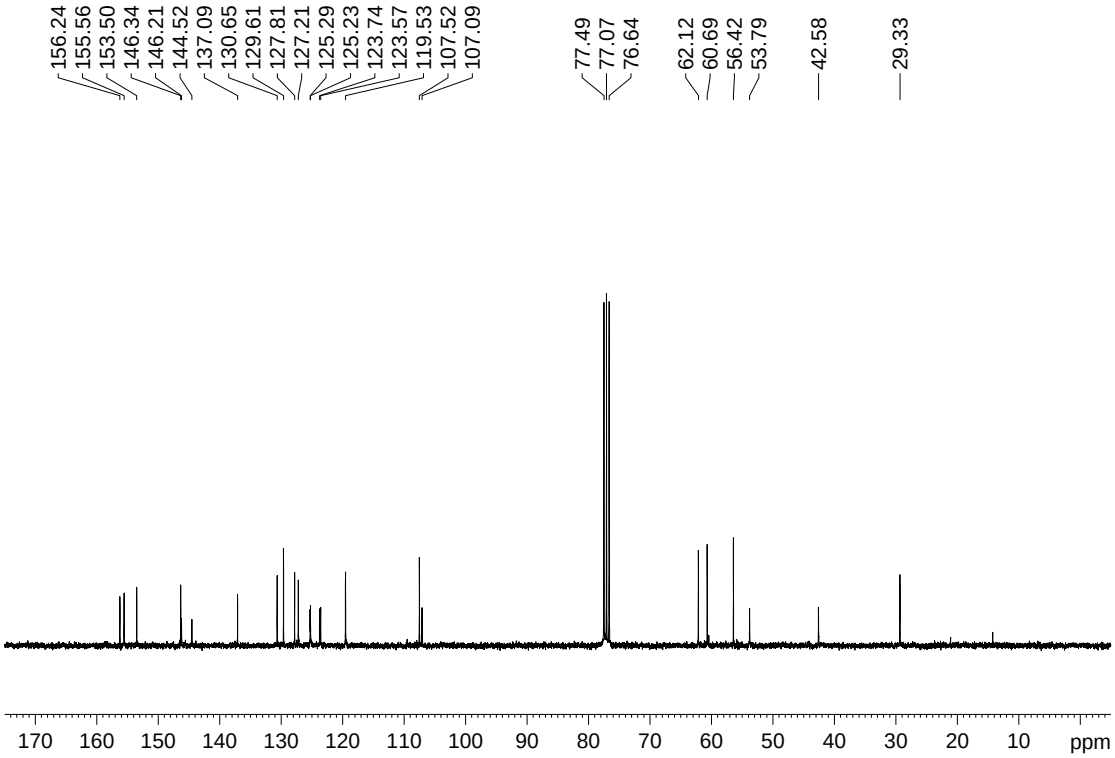

Fig. S6 ^{13}C NMR spectrum (75 MHz, $CDCl_3$) of **7**.

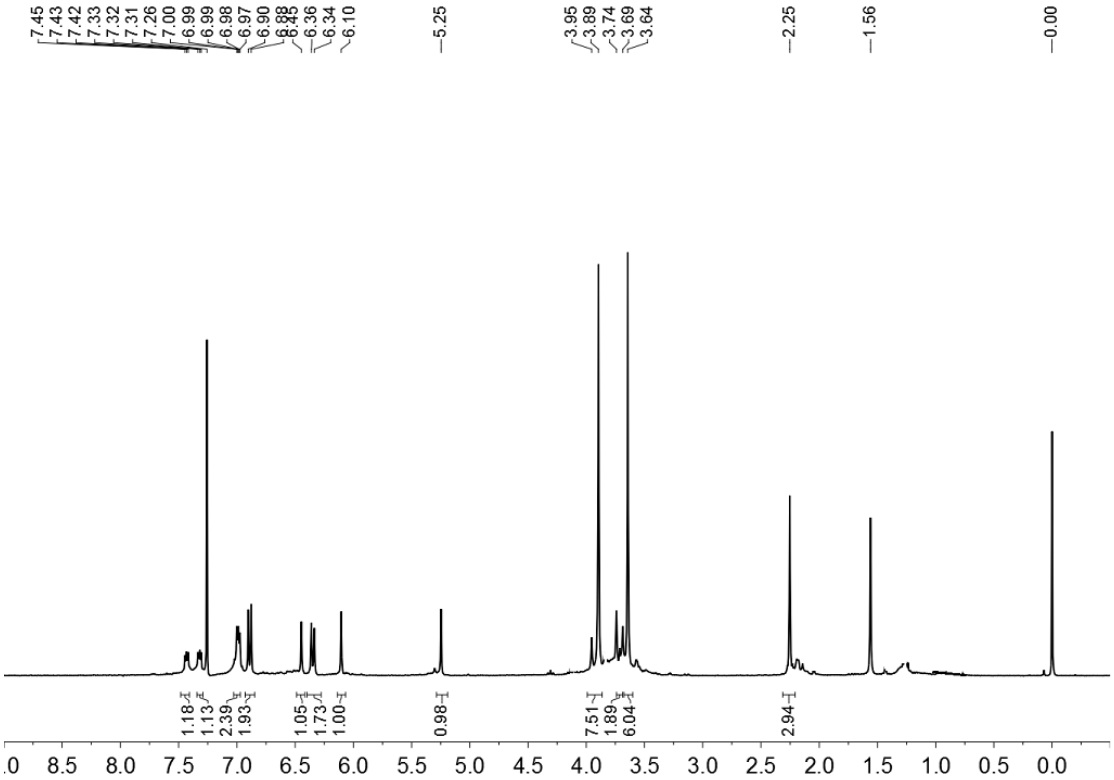

Fig. S7 ^{1}H NMR spectrum (300 MHz, $CDCl_3$) of **8a**.

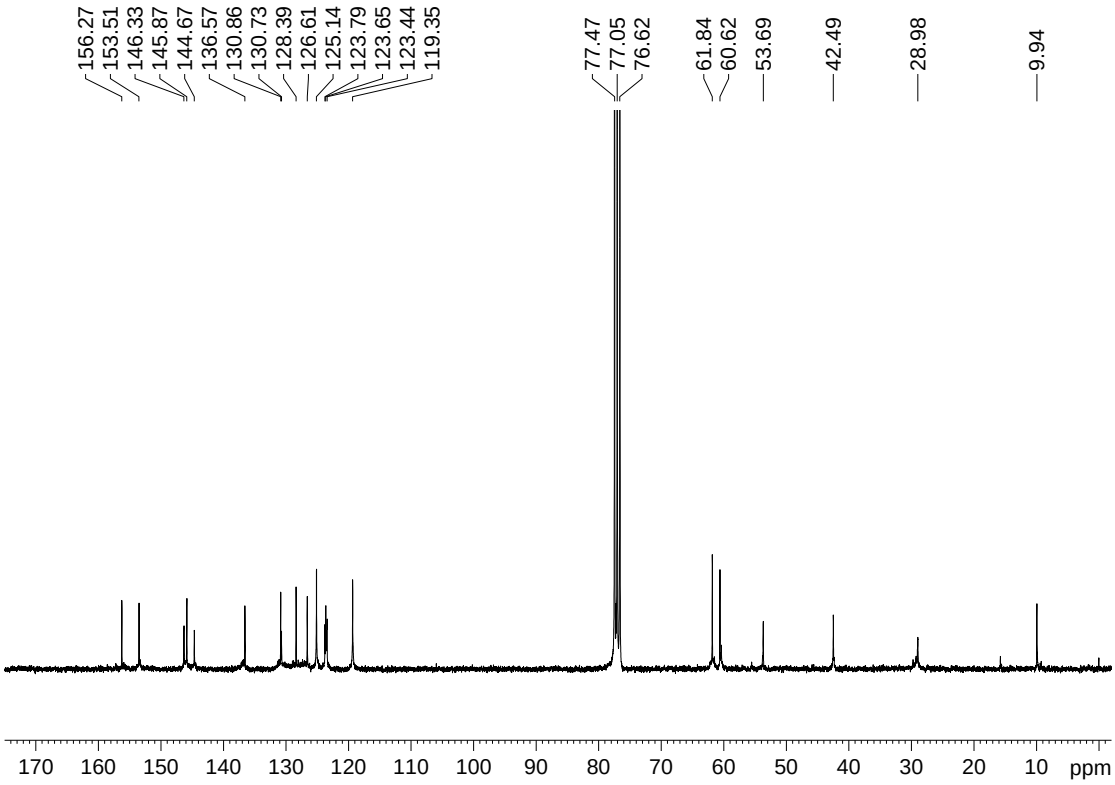

Fig. S8 ^{13}C NMR spectrum (75 MHz, $CDCl_3$) of **8a**.

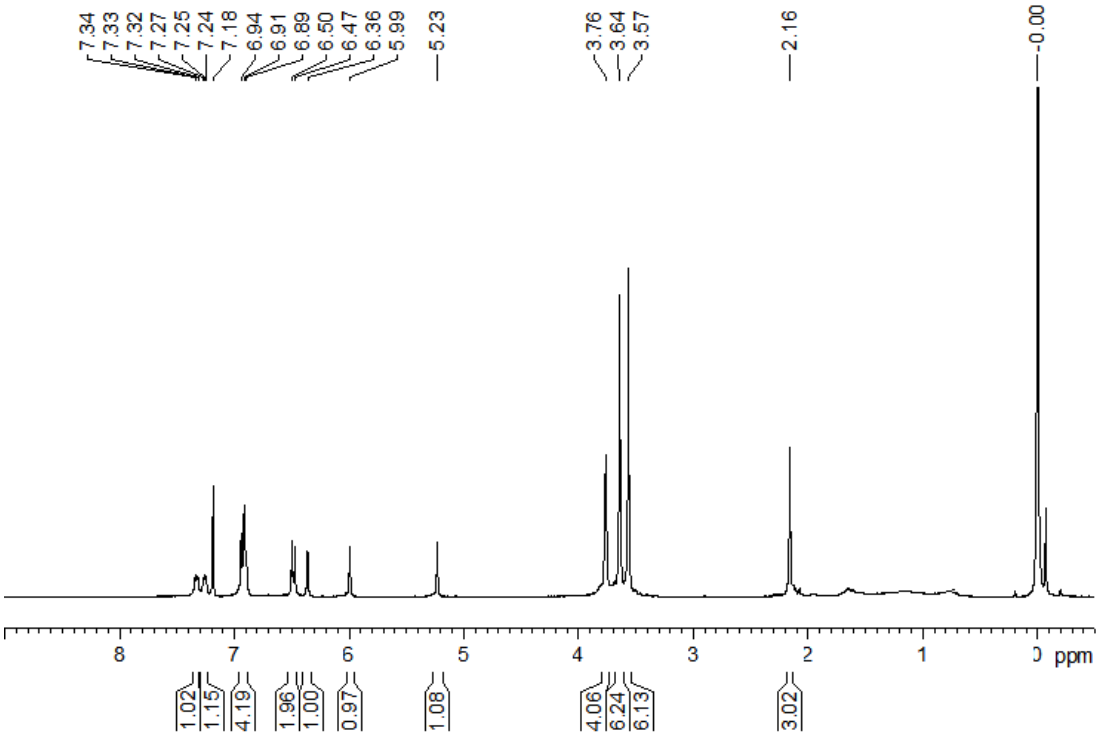

Fig. S9 ^{1}H NMR spectrum (300 MHz, $CDCl_3$) of **8b**.

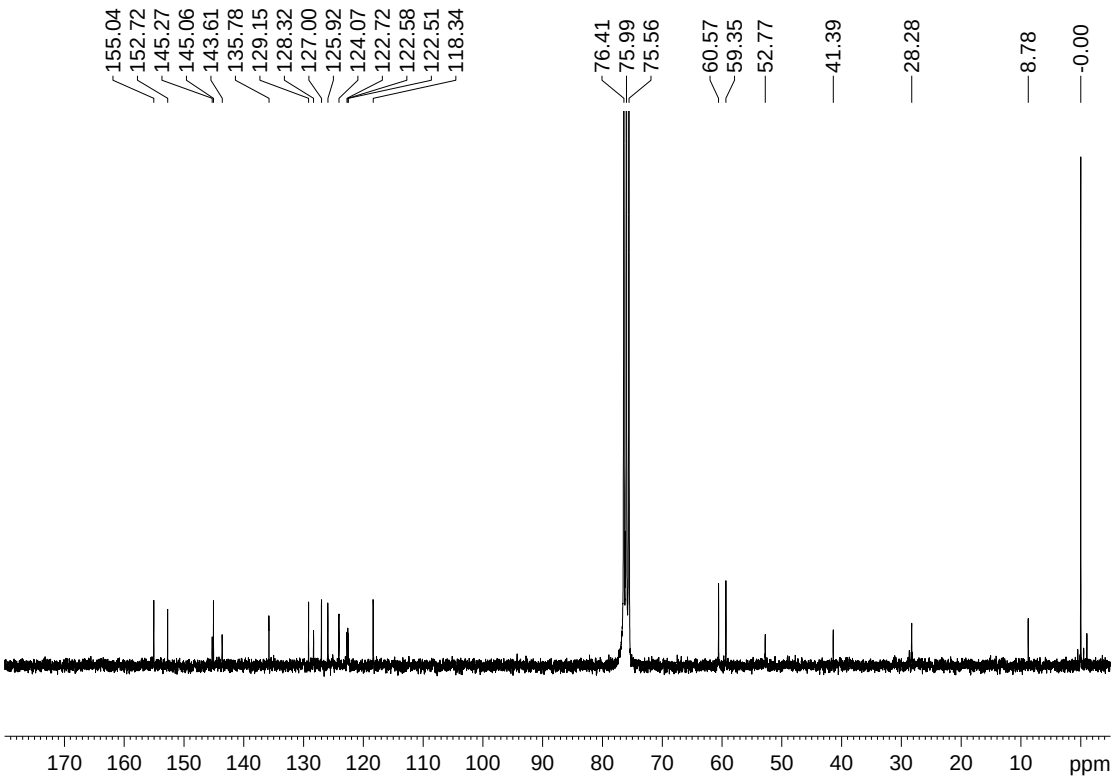

Fig. S10 ^{13}C NMR spectrum (75 MHz, $CDCl_3$) of **8b**.

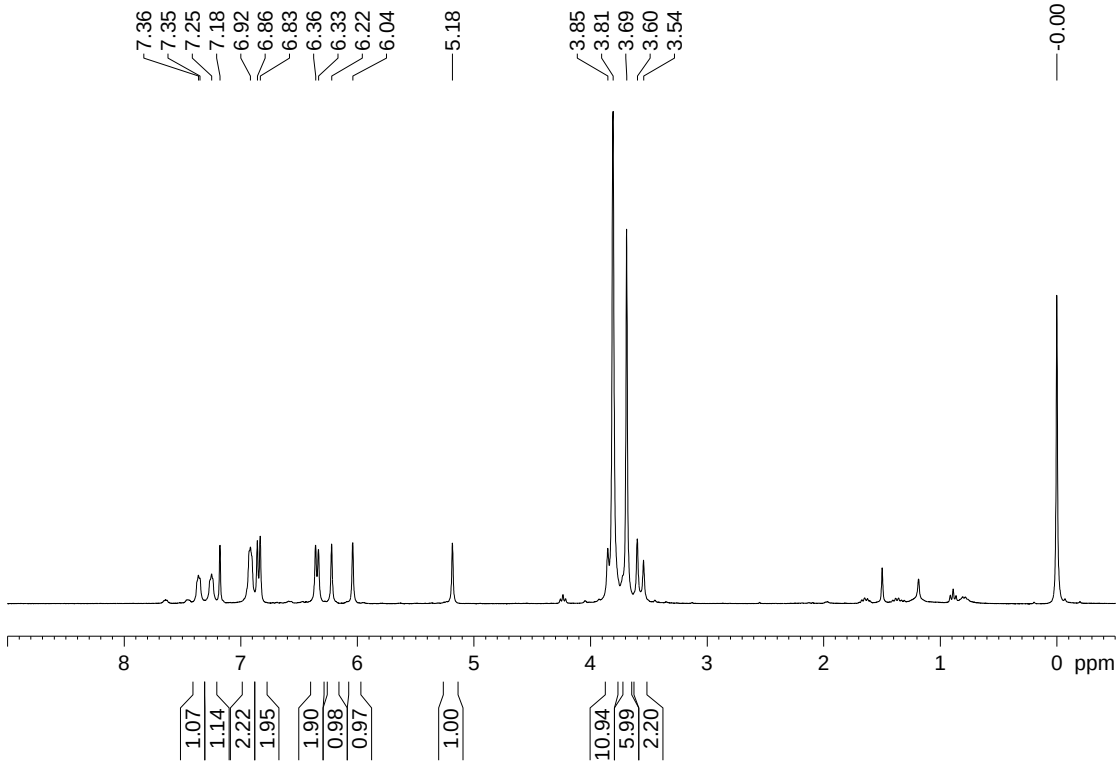

Fig. S11 ^{1}H NMR spectrum (300 MHz, $CDCl_3$) of **9a**.

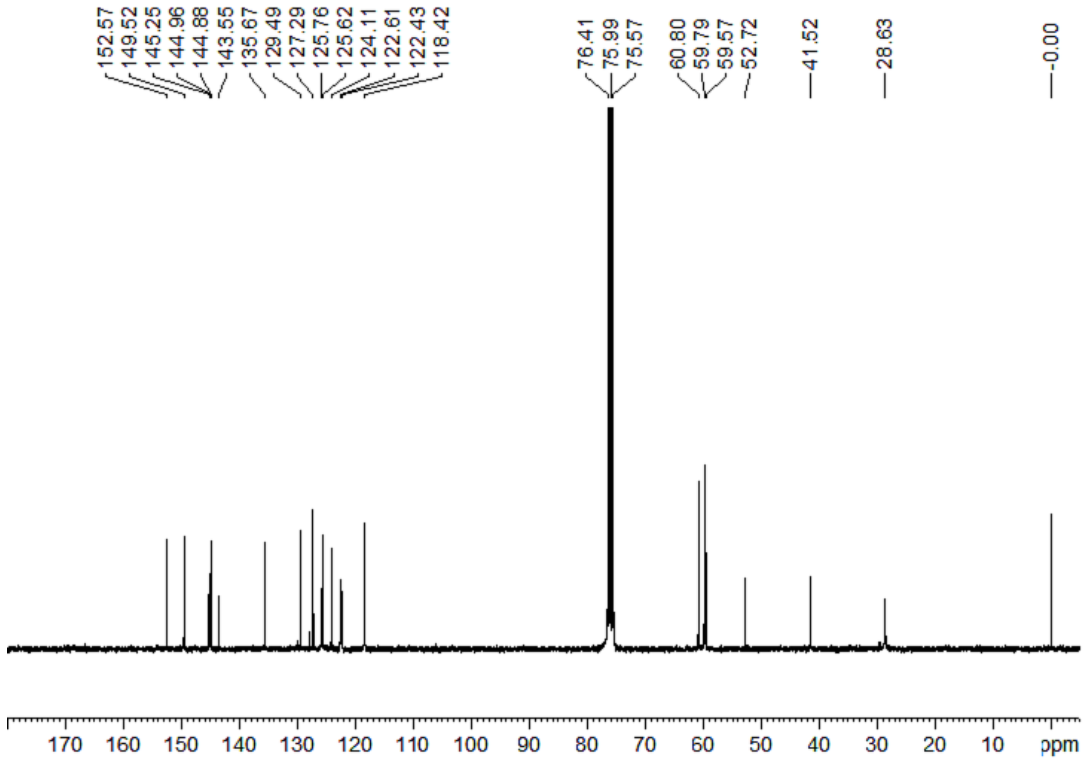

Fig. S12 ^{13}C NMR spectrum (75 MHz, $CDCl_3$) of **9a**.

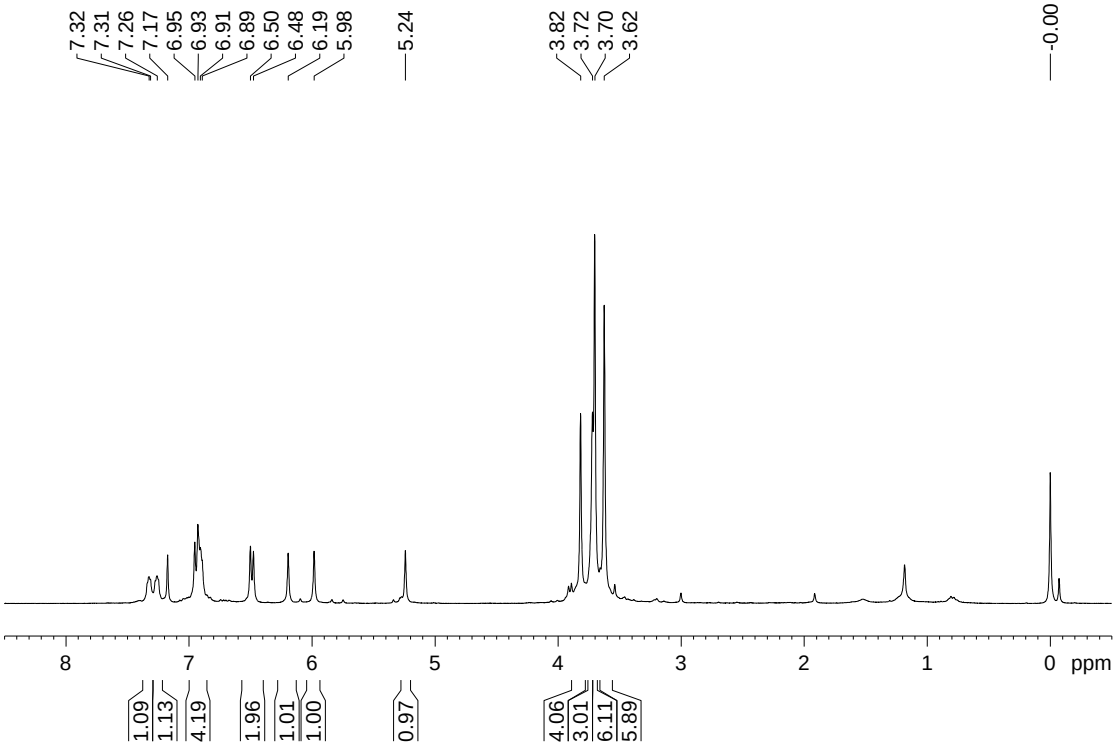

Fig. S13 ^{1}H NMR spectrum (300 MHz, $CDCl_3$) of **9b**.

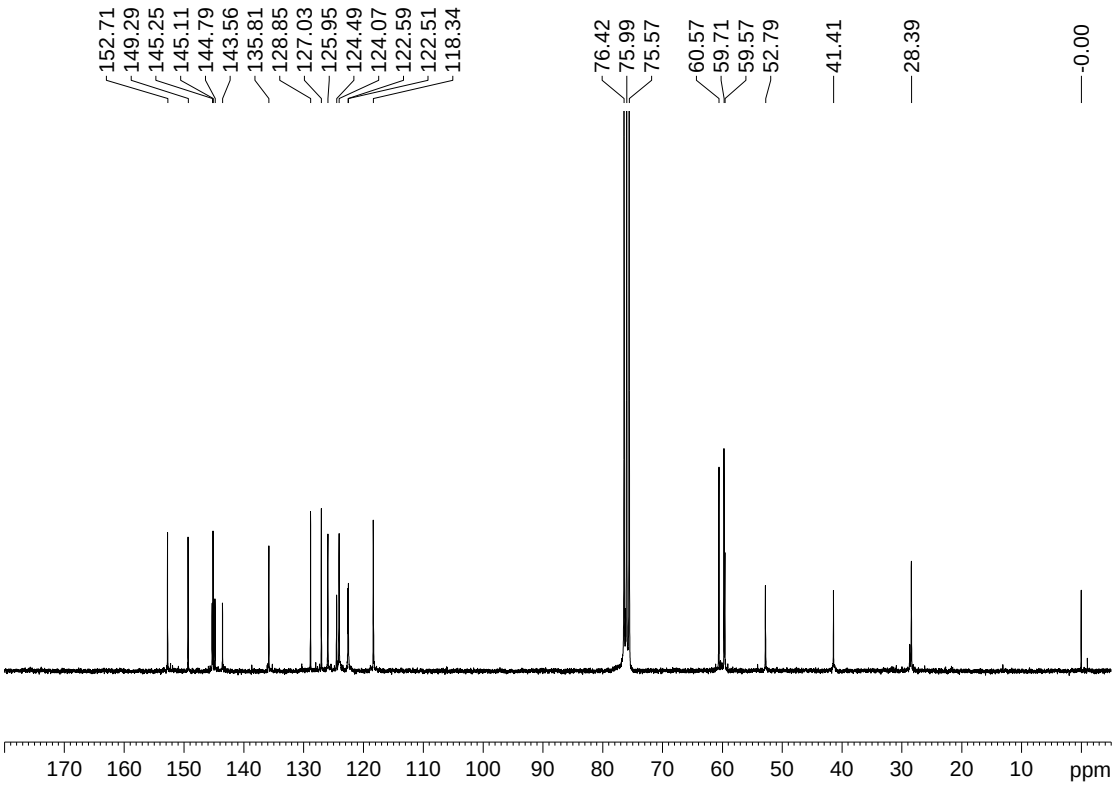

Fig. S14 ^{13}C NMR spectrum (75 MHz, $CDCl_3$) of **9b**.

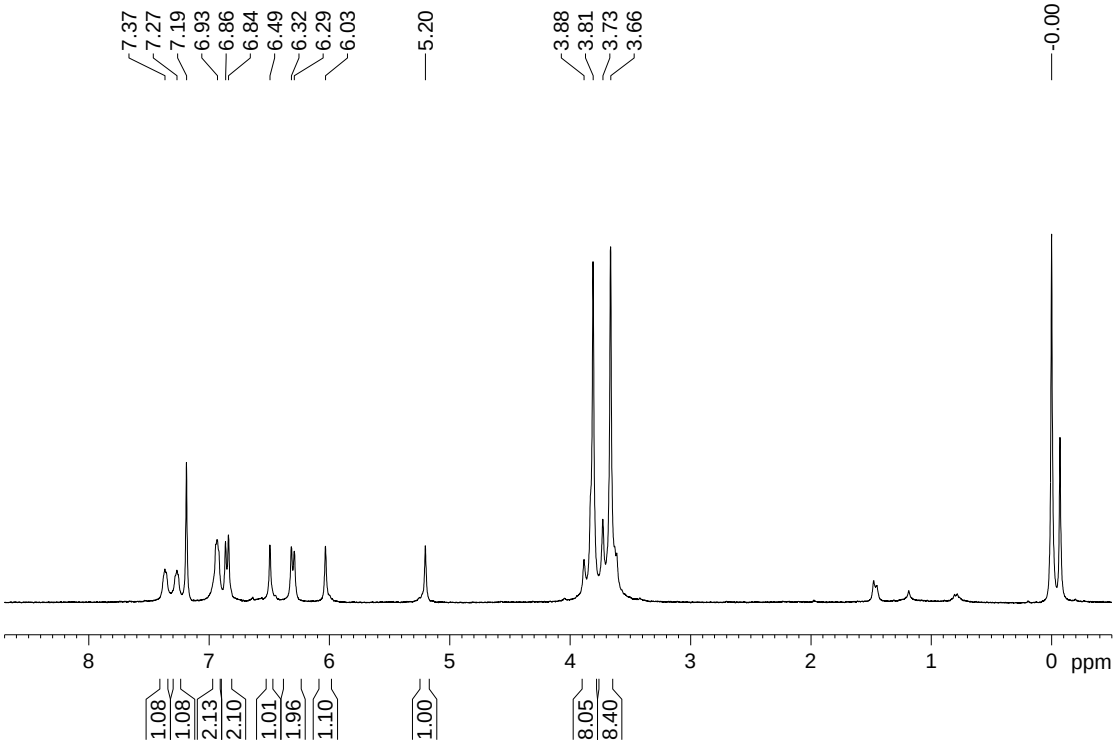

Fig. S15 ^{1}H NMR spectrum (300 MHz, $CDCl_3$) of **10a**.

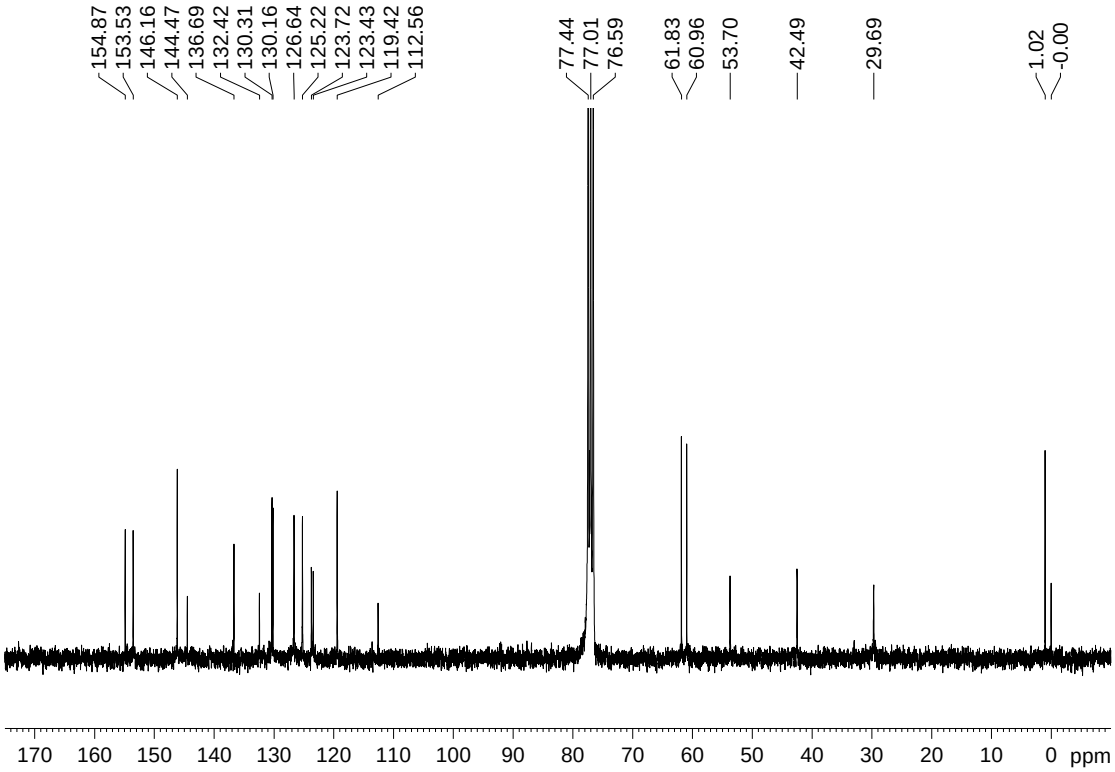

Fig. S16 ^{13}C NMR spectrum (75 MHz, $CDCl_3$) of **10a**.

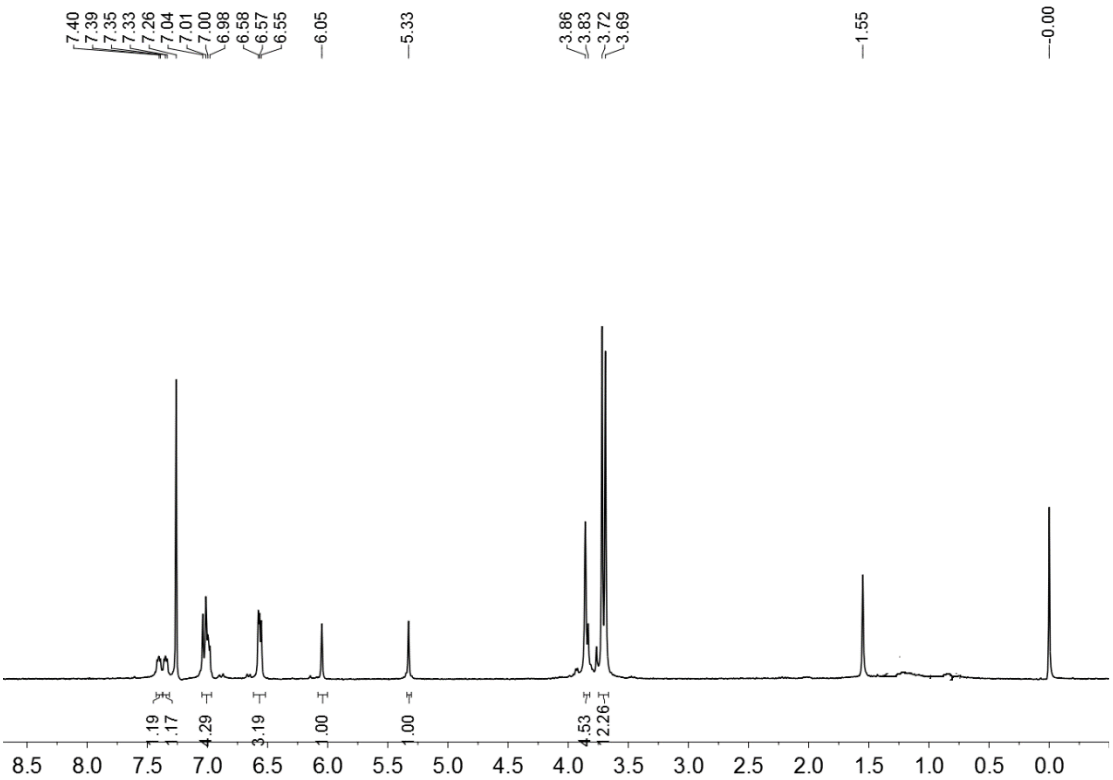

Fig. S17 ^{1}H NMR spectrum (300 MHz, $CDCl_3$) of **10b**.

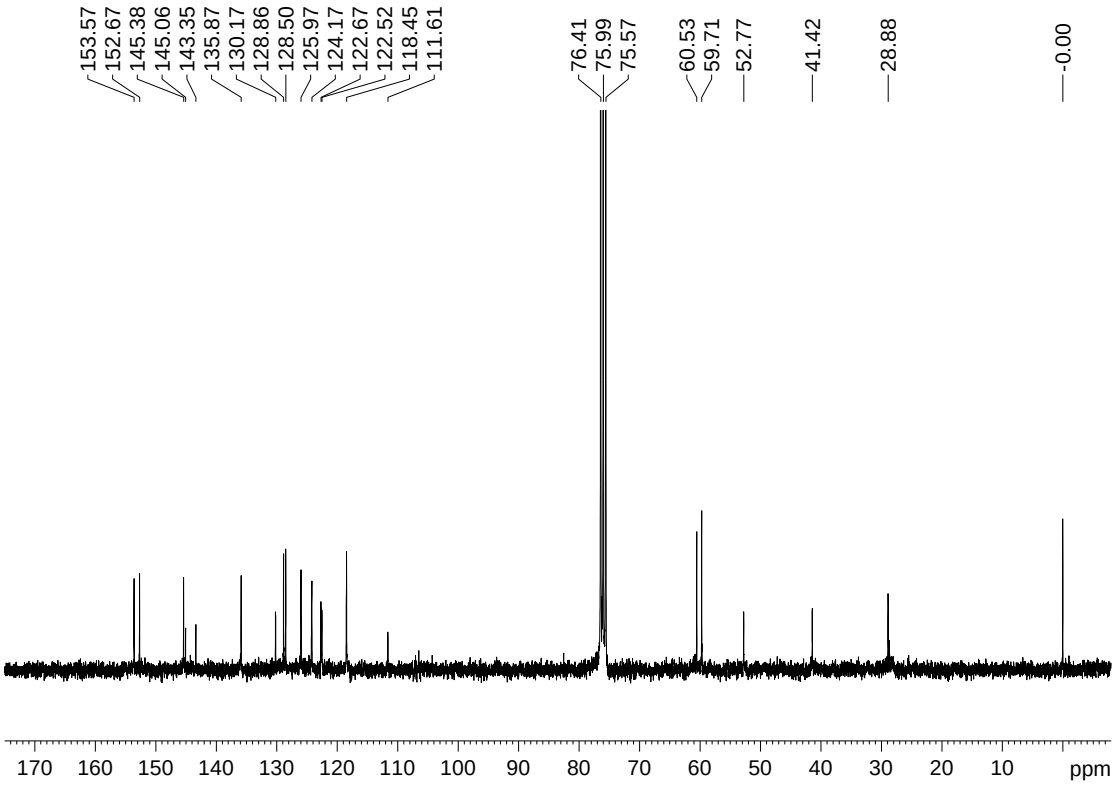

Fig. S18 ^{13}C NMR spectrum (75 MHz, $CDCl_3$) of **10b**.

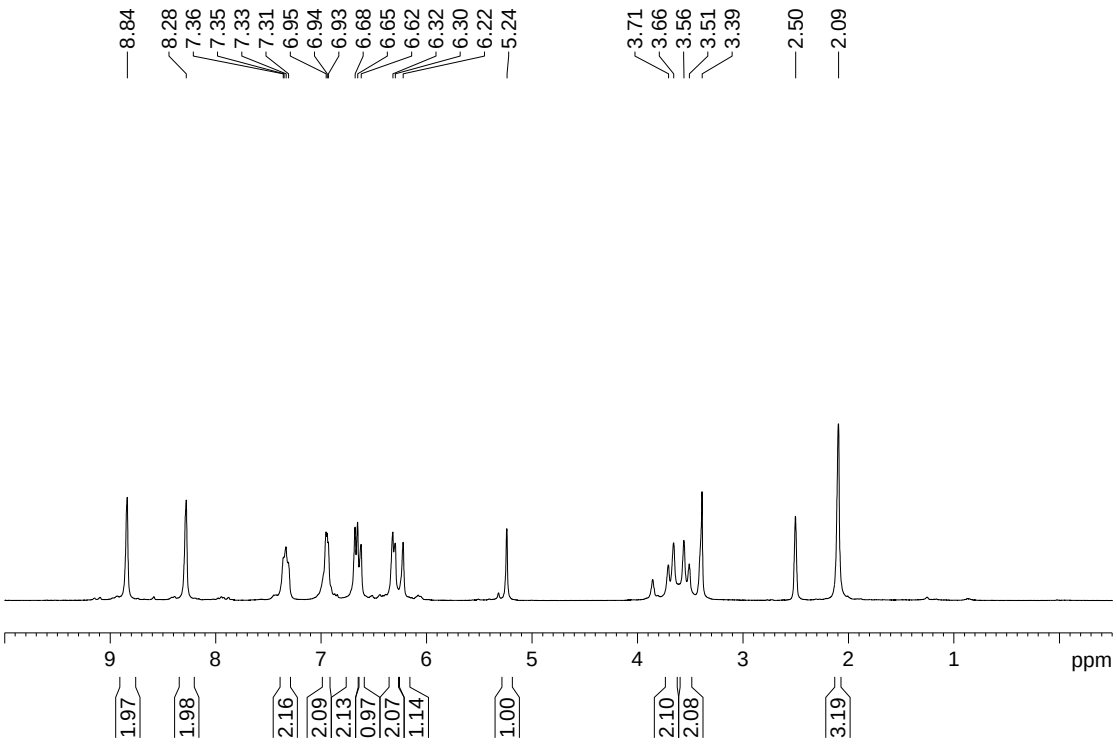

Fig. S19 ^{1}H NMR spectrum (300 MHz, DMSO-d_6) of **11a**.

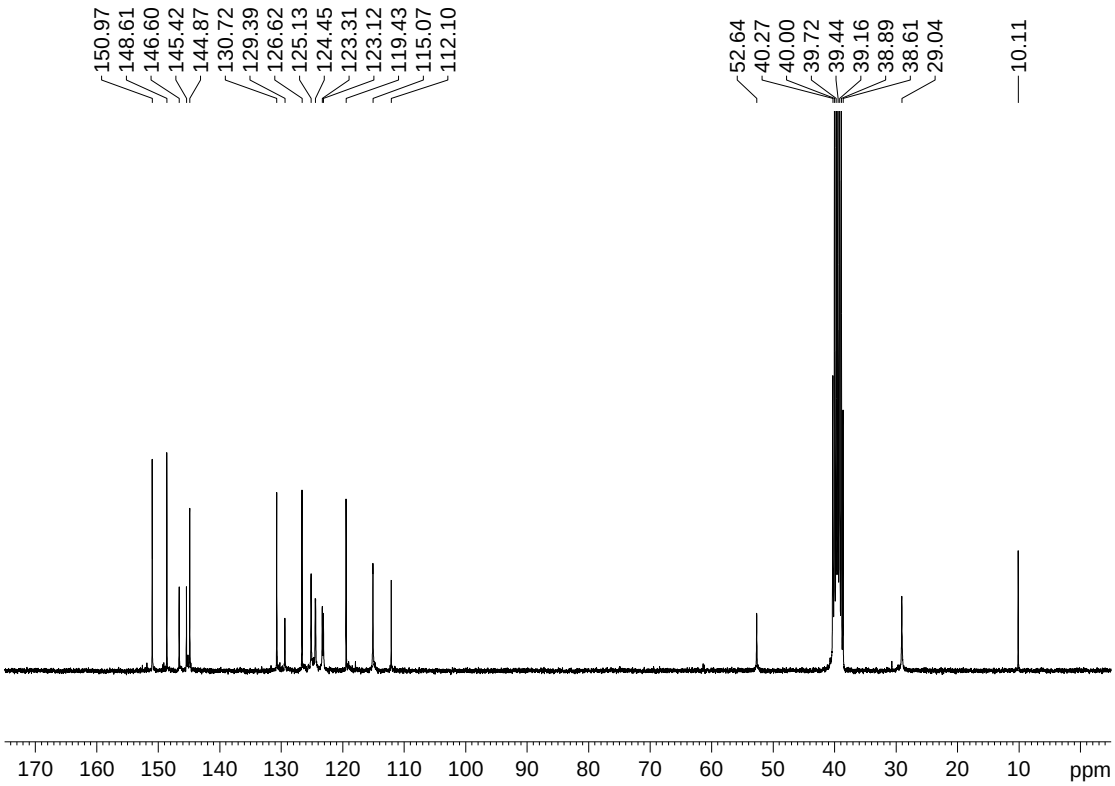

Fig. S20 ^{13}C NMR spectrum (75 MHz, DMSO-d_6) of **11a**.

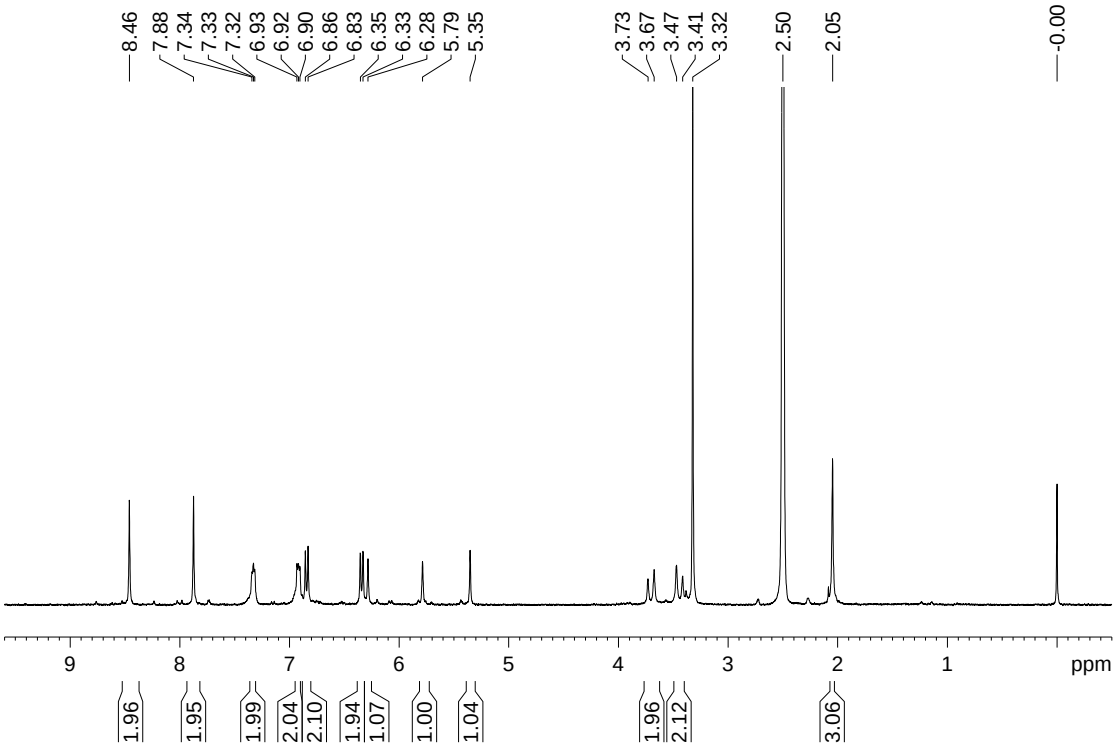

Fig. S21 ^{1}H NMR spectrum (300 MHz, DMSO-d_6) of **11b**.

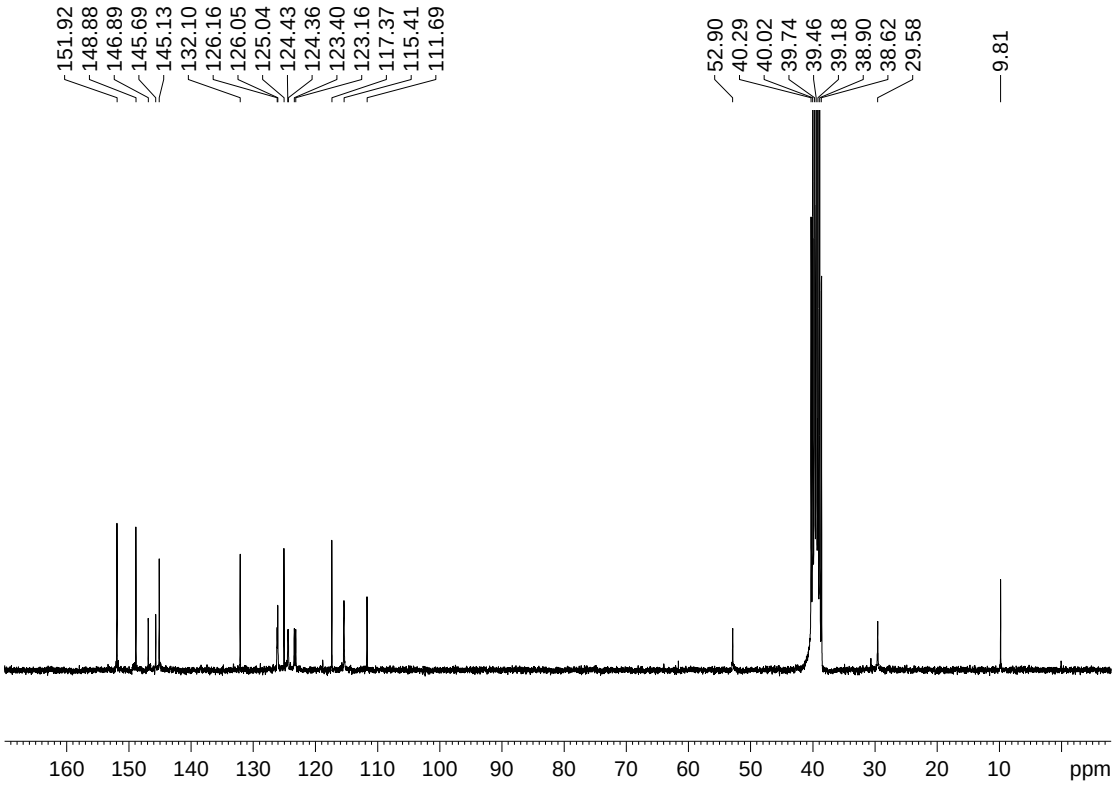

Fig. S22 ^{13}C NMR spectrum (75 MHz, DMSO-d_6) of **11b**.

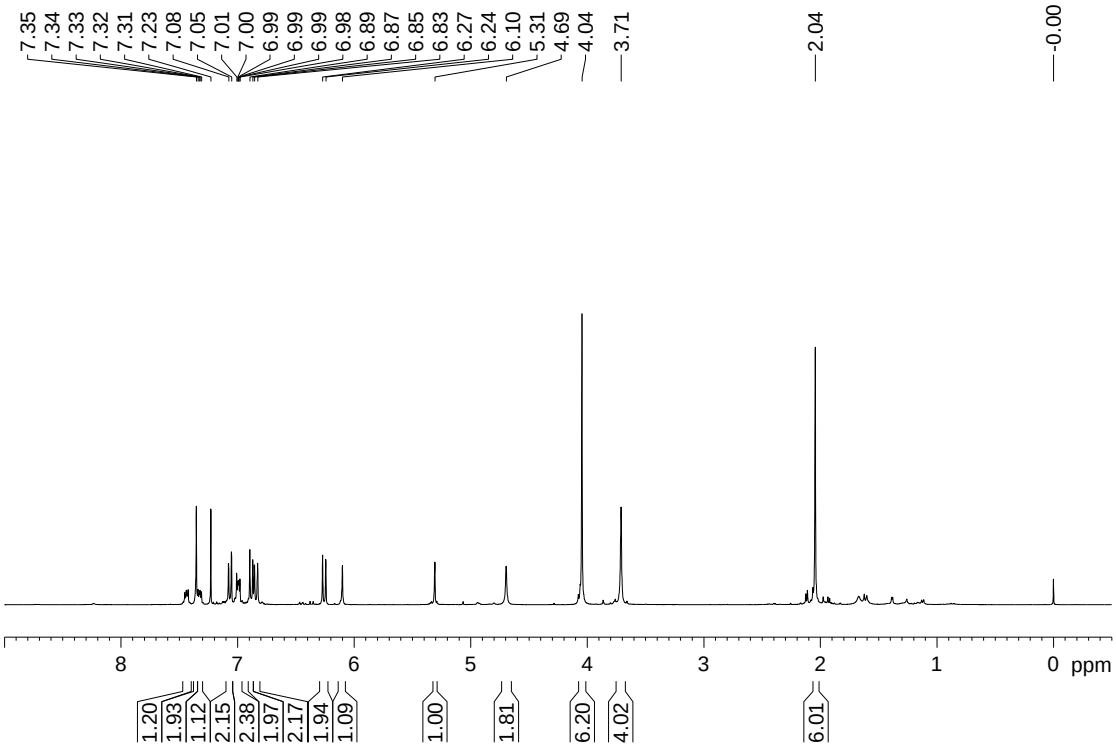

Fig. S23 ^{1}H NMR spectrum (300 MHz, $CDCl_3$) of **13**.

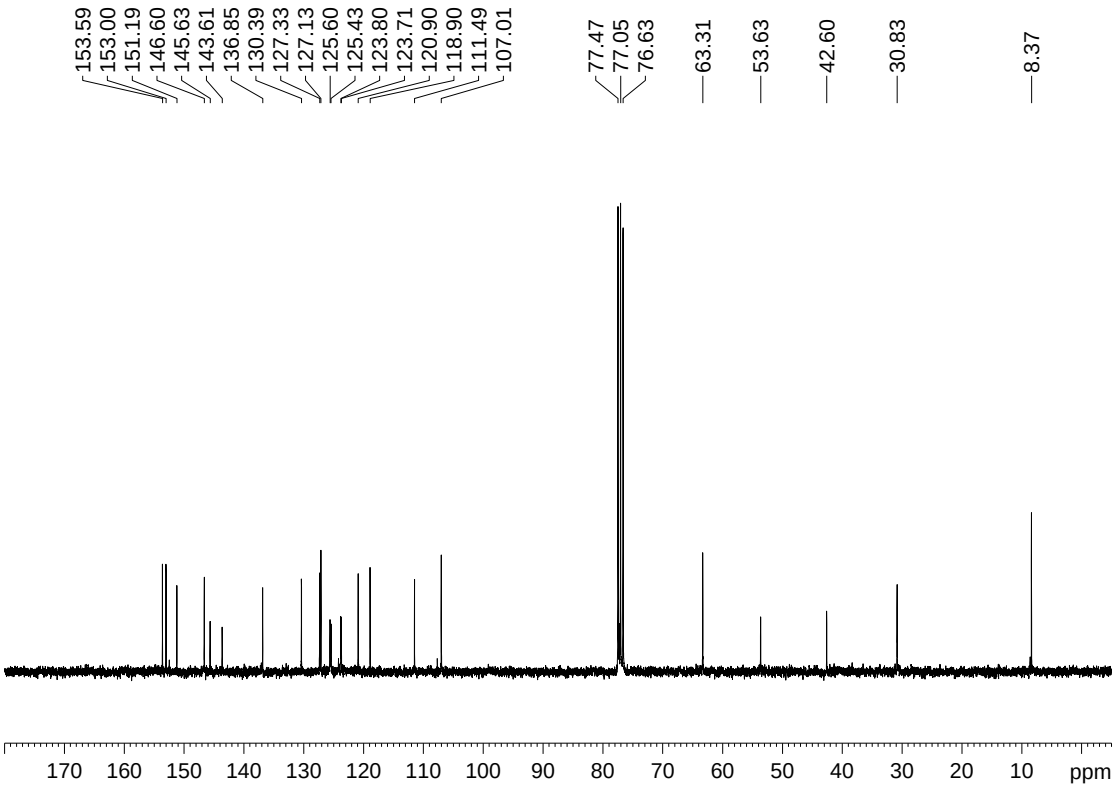

Fig. S24 ^{13}C NMR spectrum (75 MHz, $CDCl_3$) of **13**.

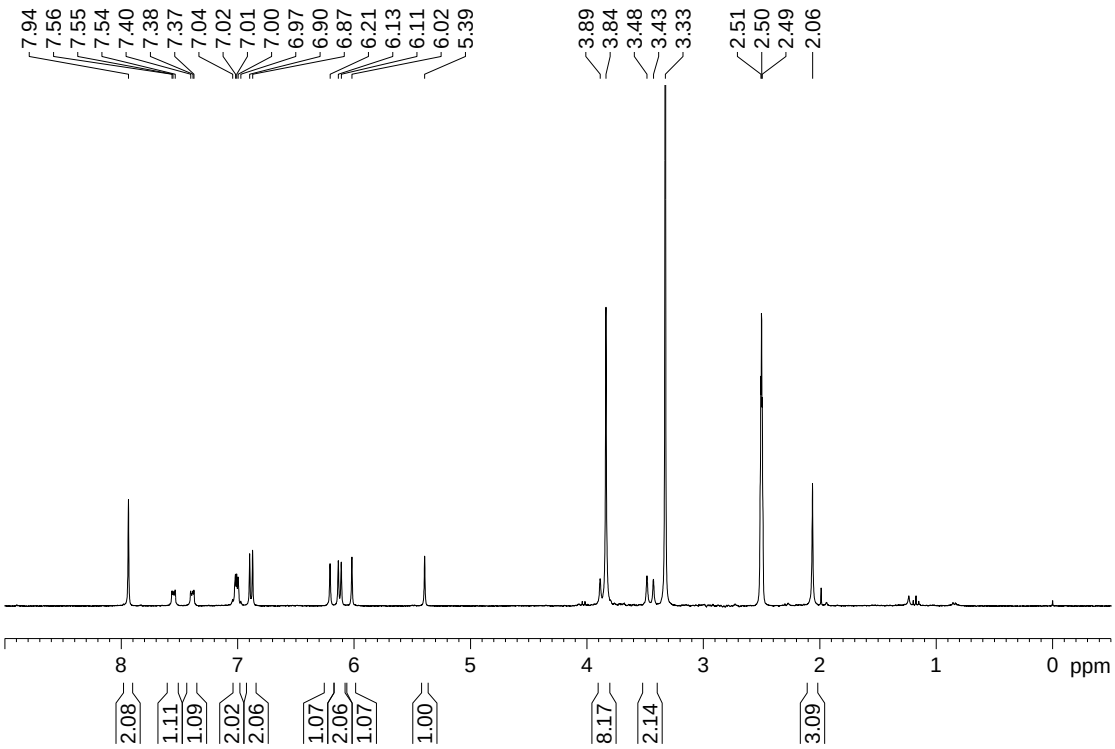

Fig. S25 ^{1}H NMR spectrum (300 MHz, DMSO-d_6) of **14a**.

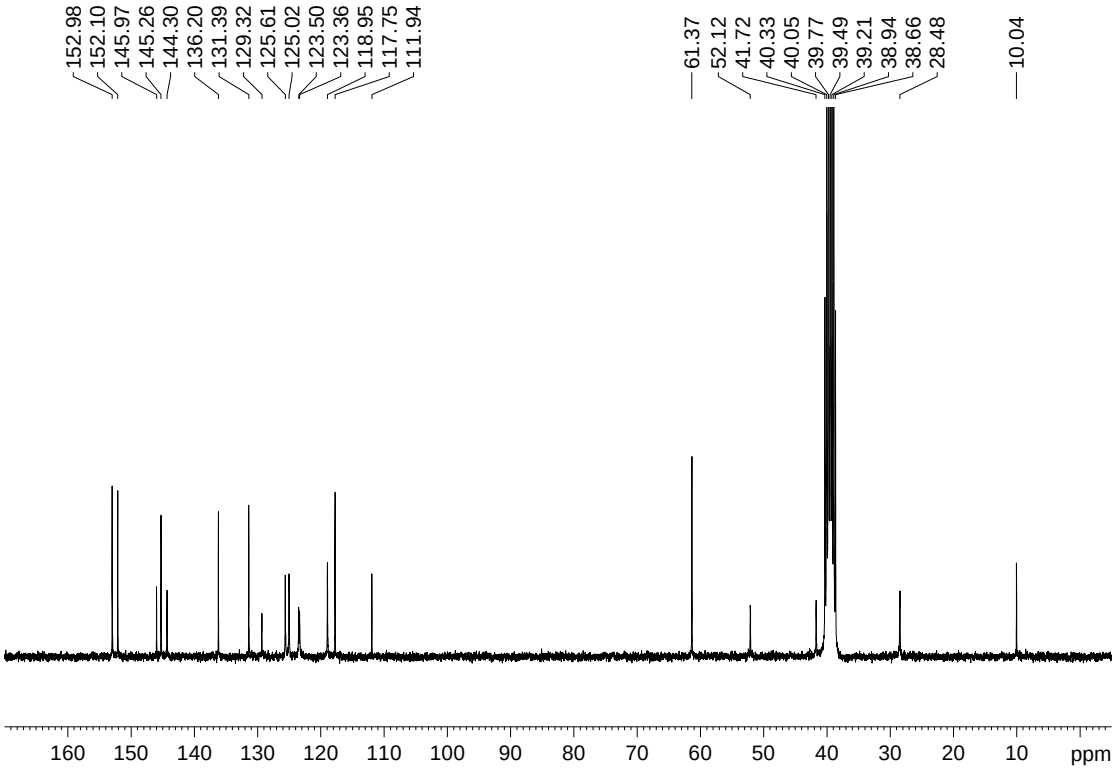

Fig. S26 ^{13}C NMR spectrum (75 MHz, DMSO-d_6) of **14a**.

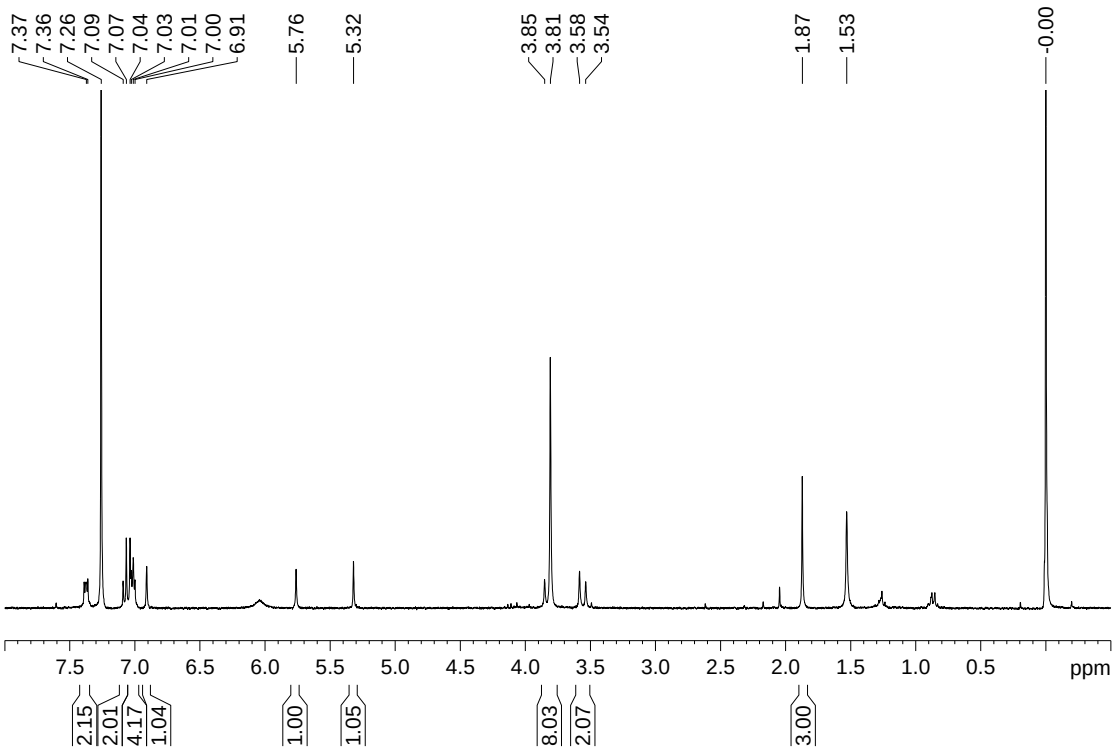

Fig. S27 ^{1}H NMR spectrum (300 MHz, $CDCl_3$) of **14b**.

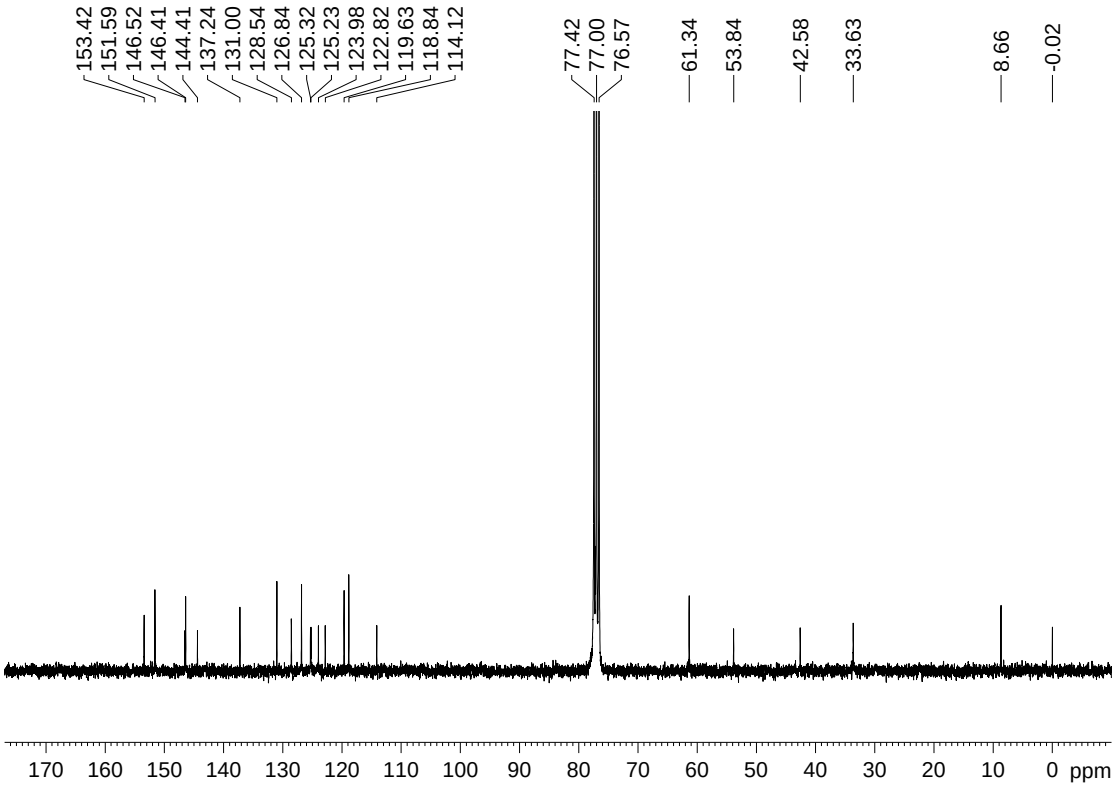

Fig. S28 ^{13}C NMR spectrum (75 MHz, $CDCl_3$) of **14b**.

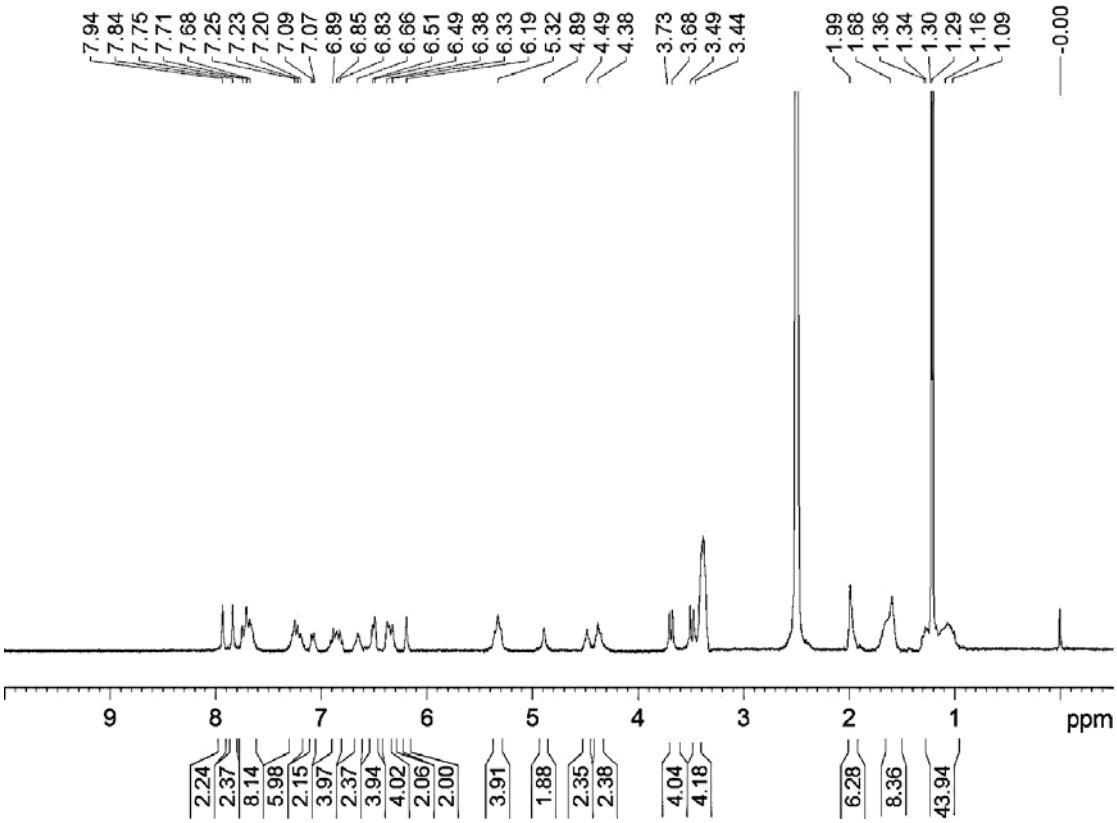

Fig. S29 ^{1}H NMR spectrum (300 MHz, DMSO-d_6) of [2]rotaxane **15**.

2. Variable-temperature ^{1}H NMR experiments of 8b, 11a, 11b and 14a

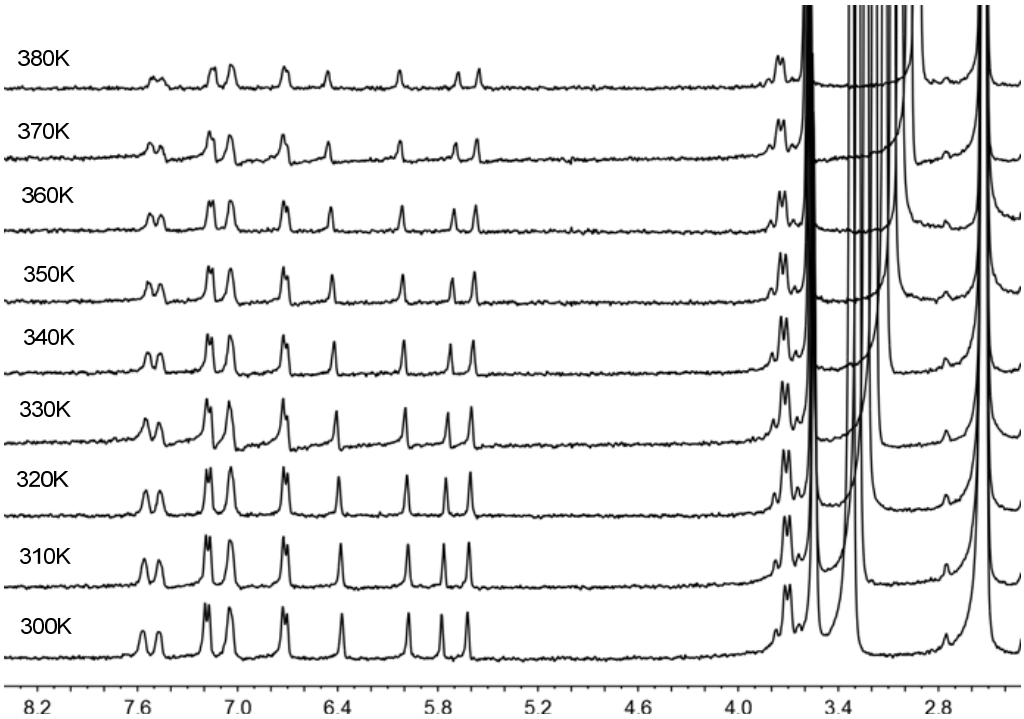

Fig. S30 Partial ^{1}H NMR spectra of **8b** (DMSO-d_6, 300MHz) at various temperatures.

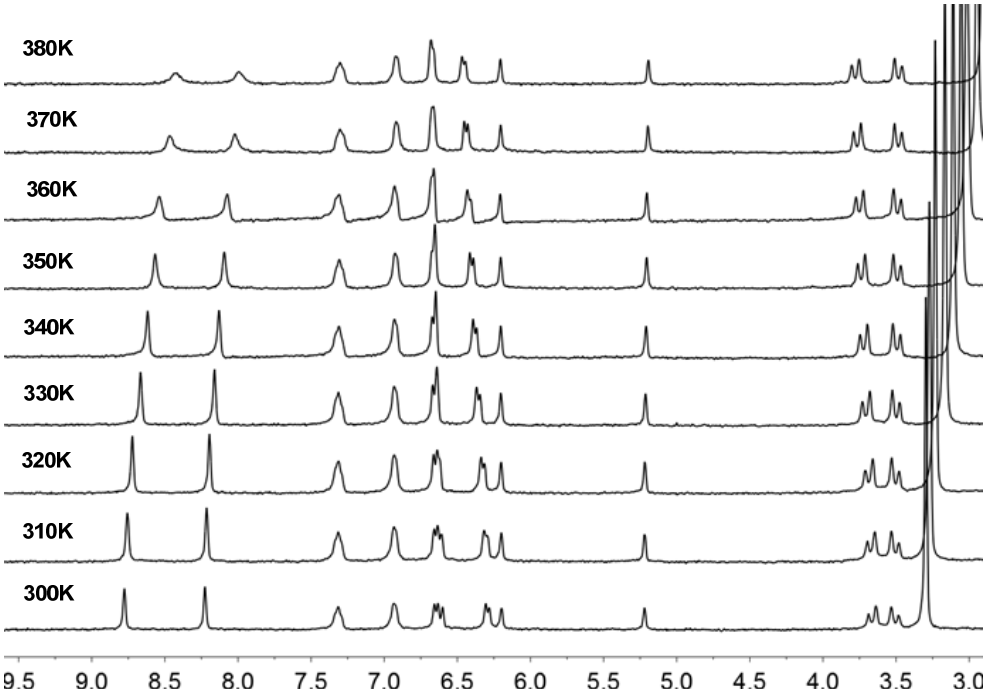

Fig. S31 Partial ^{1}H NMR spectra of **11a** (DMSO-d_6, 300MHz) at various temperatures.

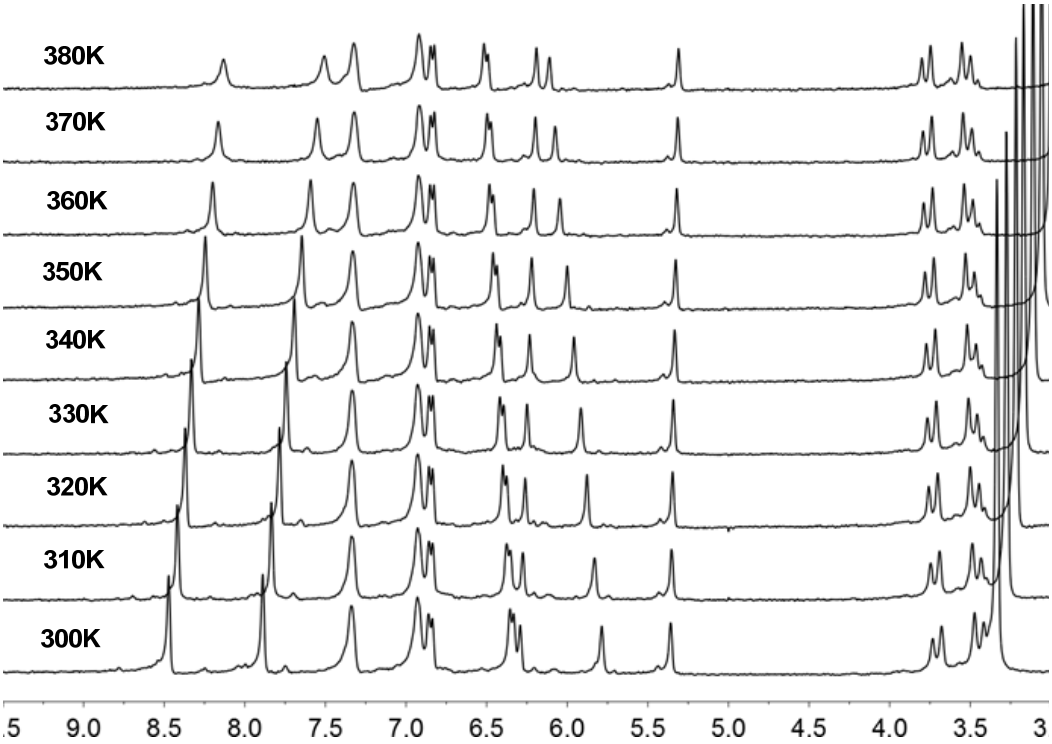

Fig. S32 Partial ^{1}H NMR spectra of **11b** (DMSO-d_6, 300MHz) at various temperatures.

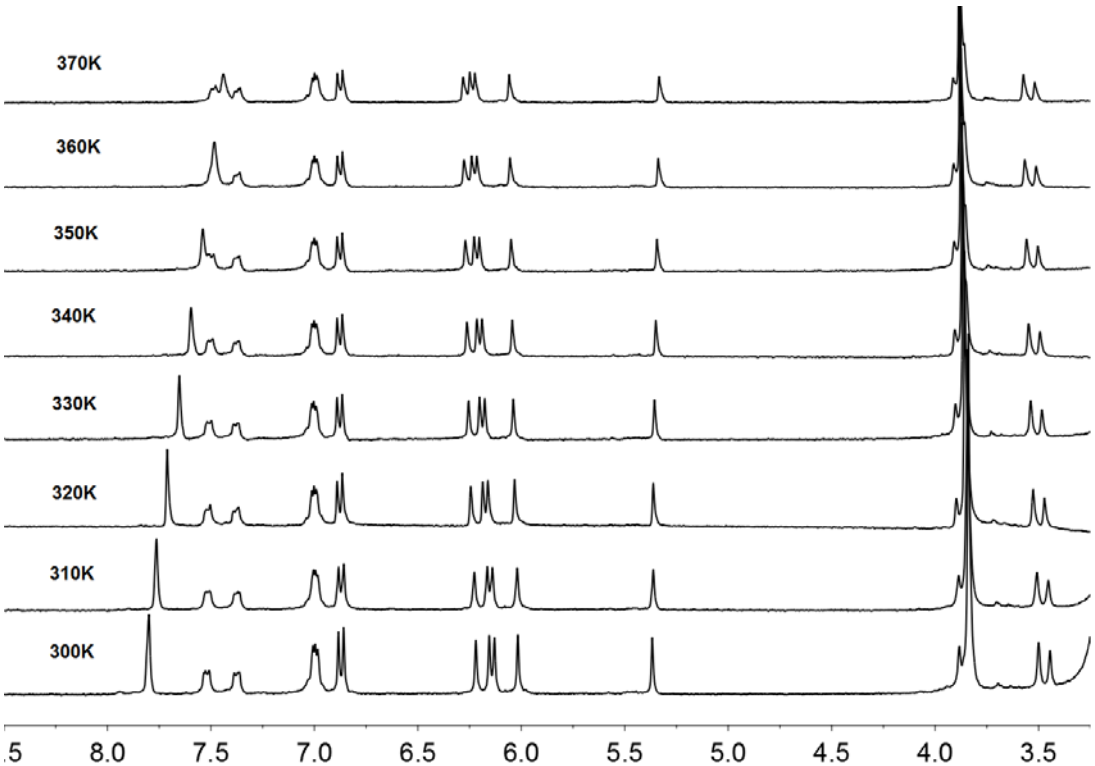

Fig. S33 Partial ^{1}H NMR spectra of **14a** (DMSO-d_6, 300MHz) at various temperatures.

3. X-ray crystal data and packing of 8a, 8b, 9b, 10b, and 14a

Crystal Data for **8a**: $C_{74}H_{72}O_{12}$, M_w = 1153.32, crystal size 0.32 × 0.15 × 0.13 mm, Orthorhombic, space group *Pccn*, a = 17.548(4), b = 24.274(5), c = 14.468(3) Å, α = 90°, β = 90°, γ = 90°, V = 6163(2) Å^3, Z = 4, D = 1.243 Mg m^{-3}, T = 173(2) K, 36553 reflections measured, 5417 unique (R_{int} = 0.0863), final R indices [$I > 2\sigma(I)$]: R_1 = 0.1251, wR_2 = 0.3265, R indices (all data): R_1 = 0.1395, wR_2 = 0.3503. CCDC 931895.

Crystal Data for **8b**·2$CHCl_3$: $C_{68}H_{62}Cl_6O_8$, M_w = 1219.88, crystal size 0.43 × 0.34 × 0.30 mm, Triclinic, space group *P*-1, a = 11.466(2), b = 11.708(2), c = 13.256(3) Å, α = 69.828(9)°, β = 73.892(9)°, γ = 72.609(9)°, V = 1563.5(6) Å^3, Z = 1, D = 1.296 Mg m^{-3}, T = 173(2) K, 16948 reflections measured, 5487 unique (R_{int} = 0.0395), final R indices [$I > 2\sigma(I)$]: R_1 = 0.0849, wR_2 = 0.2311, R indices (all data): R_1 = 0.0925, wR_2 = 0.2403. CCDC 931896.

Crystal Data for **9b**: $C_{66}H_{60}O_{10}$, M_w = 1013.14, crystal size 0.32 × 0.31 × 0.08 mm, Triclinic, space group *P*-1, a = 11.429(2), b = 11.955(2), c = 12.714(3) Å, α = 72.18(3)°, β = 70.44(3)°, γ = 70.84(3)°, V = 1508.3(5) Å^3, Z = 1, D = 1.115 Mg m^{-3}, T = 173(2) K, 19654 reflections measured, 6896 unique (R_{int} = 0.0486), final R indices [$I > 2\sigma(I)$]: R_1 = 0.0974, wR_2 = 0.2766, R indices (all data): R_1 = 0.1111, wR_2 = 0.2907. CCDC 931897.

Crystal Data for **10b**·2CH_2Cl_2: $C_{66}H_{58}Br_2Cl_4O_8$, M_w = 1280.74, crystal size 0.31 × 0.30 × 0.06 mm, Triclinic, space group *P*-1, a = 11.493(2), b = 11.851(2), c = 12.708(3) Å, α = 71.48(3)°, β = 71.12(3)°, γ = 72.93(3)°, V = 1517.4(5) Å^3, Z = 1, D = 1.402 Mg m^{-3}, T = 173(2) K, 16886 reflections measured, 5342 unique (R_{int} = 0.0811), final R indices [$I > 2\sigma(I)$]: R_1 = 0.0920, wR_2 = 0.2566, R indices (all data): R_1 = 0.1100, wR_2 = 0.2809. CCDC 931898.

Crystal Data for **14a**·5$CHCl_3$: $C_{67}H_{57}Cl_{15}O_8$, M_w = 1521.88, crystal size 0.63 x 0.59 x 0.09 mm, Monoclinic, space group *P2(1)/c*, a = 21.999(4), b = 19.134(4), c = 33.115(7) Å, α = 90°, β = 98.09(3)°, γ = 90°, V = 13800(5) Å^3, Z = 8, D = 1.465 Mg m^{-3}, T = 173(2) K, 79446 reflections measured, 24153 unique (R_{int} = 0.0773), final R indices [$I > 2\sigma(I)$]: R_1 = 0.1658, wR_2 = 0.3414, R indices (all data): R_1 = 0.1855, wR_2 = 0.3536. CCDC 931783.

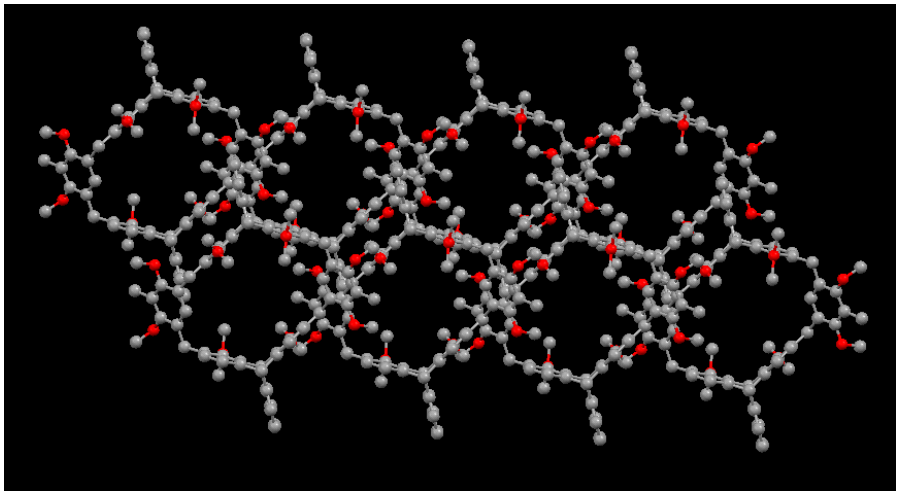

Fig. S34 A 3D microporous structure of **8b** viewed along the *c*-axis. Solvent molecules and hydrogen atoms were omitted for clarity.

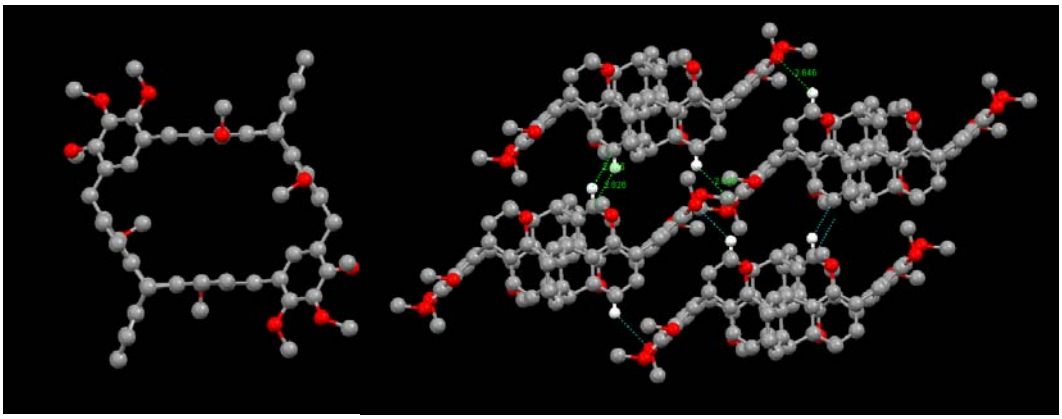

Fig. S35 Crystal structure of **9b** viewed along the *c*-axis. Solvent molecules and hydrogen atoms were omitted for clarity.

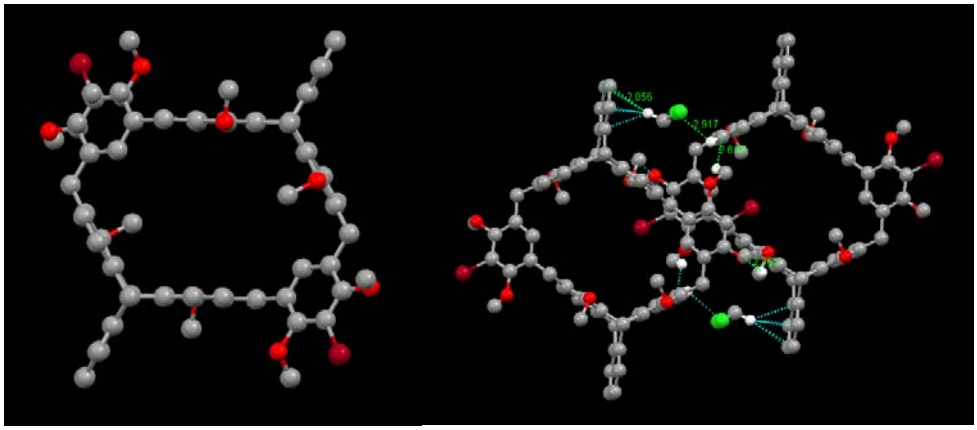

Fig. S36 Top view of crystal structure of **10b**, and solvent molecules and hydrogen atoms were omitted for clarity.

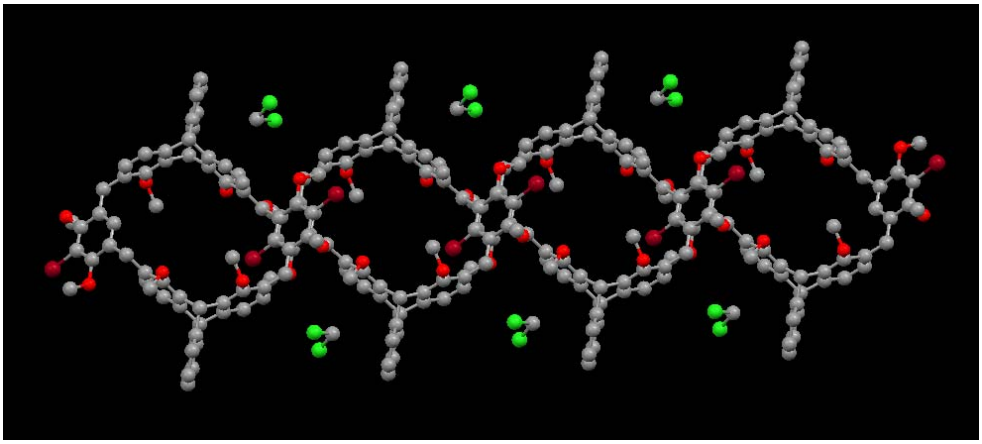

Fig. S37 A 2D layer structure of macrocycle **10b** with the CH_2Cl_2 molecules situated inside the exterior of the cavity.

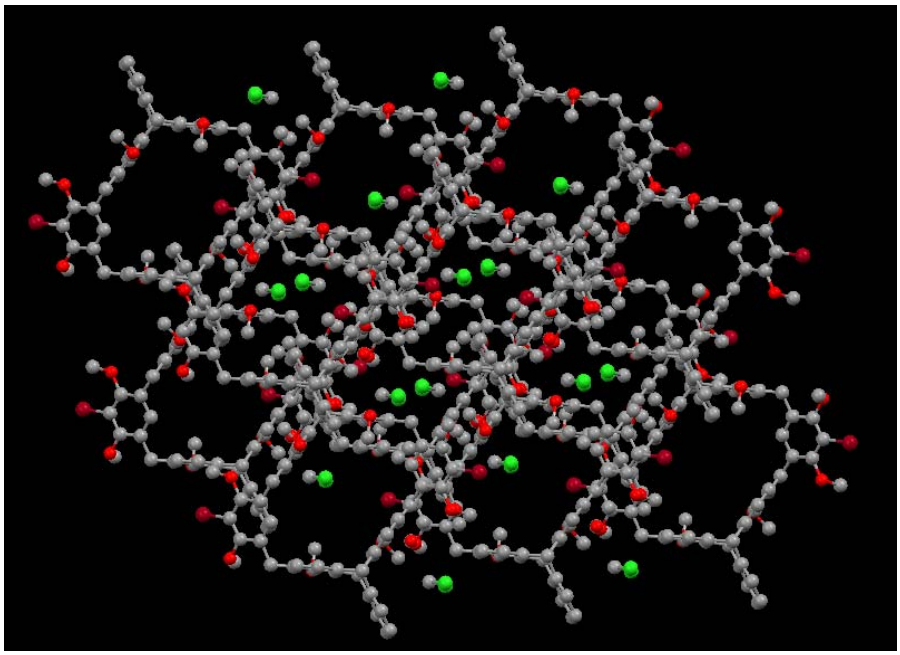

Fig. S38 A 3D microporous structure of macrocycle **10b** viewed along the *c*-axis. The CH_2Cl_2 molecules situated in the different channels and hydrogen atoms are omitted for clarity.

4. The comparison of ^{1}H NMR spectra between host 11a and the guests

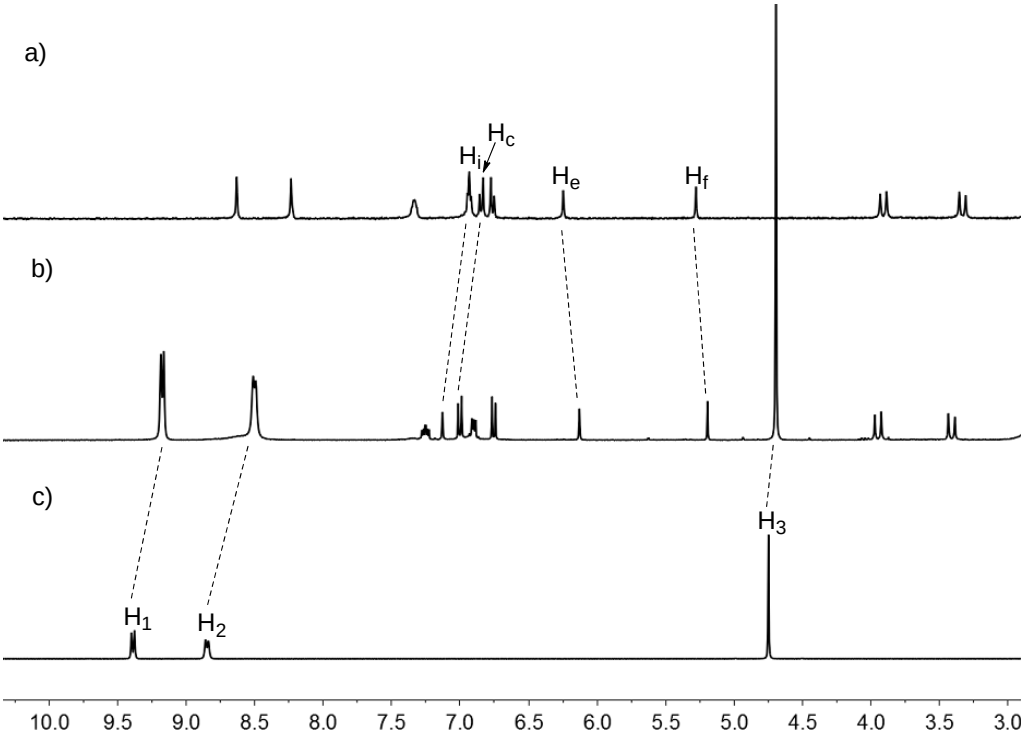

Fig. S39 Partial ^{1}H NMR spectra (300 MHz, acetone-d_6, 298 K) of (a) free host **11a**, (b) host **11a** with 1.0 equiv of **G1** and (c) free guest **G1**. [**11a**]$_0$ = 2.0 mM.

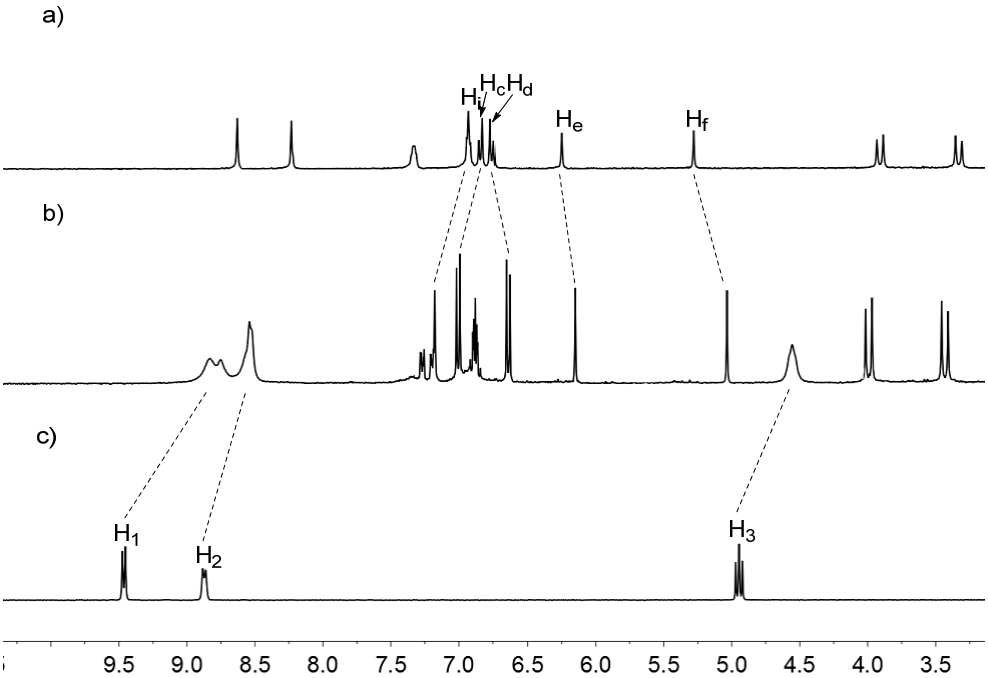

Fig. S40 Partial ^{1}H NMR spectra (300 MHz, Acetone-d_6, 298 K) of (a) free host **11a**, (b) host **11a** with 1.0 equiv of **G2** and (c) free guest **G2**. [**11a**]$_0$ = 2.0 mM.

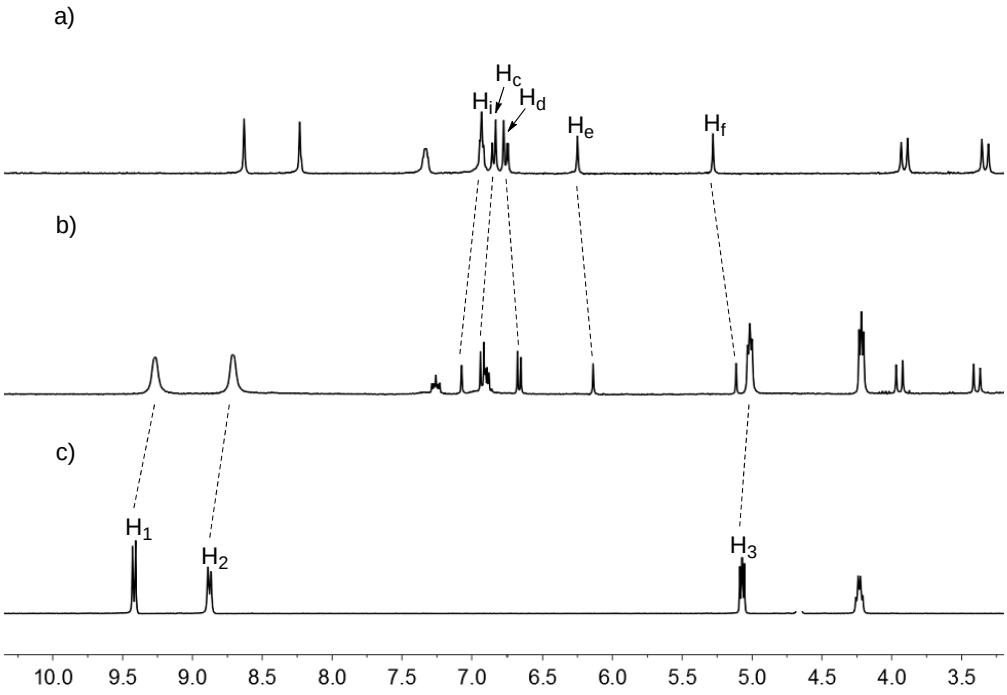

Fig. S41 Partial ^{1}H NMR spectra (300 MHz, acetone-d_6, 298 K) of (a) free host **11a**, (b) host **11a** with 1.0 equiv of **G3** and (c) free guest **G3**. [**11a**]$_0$ = 2.0 mM.

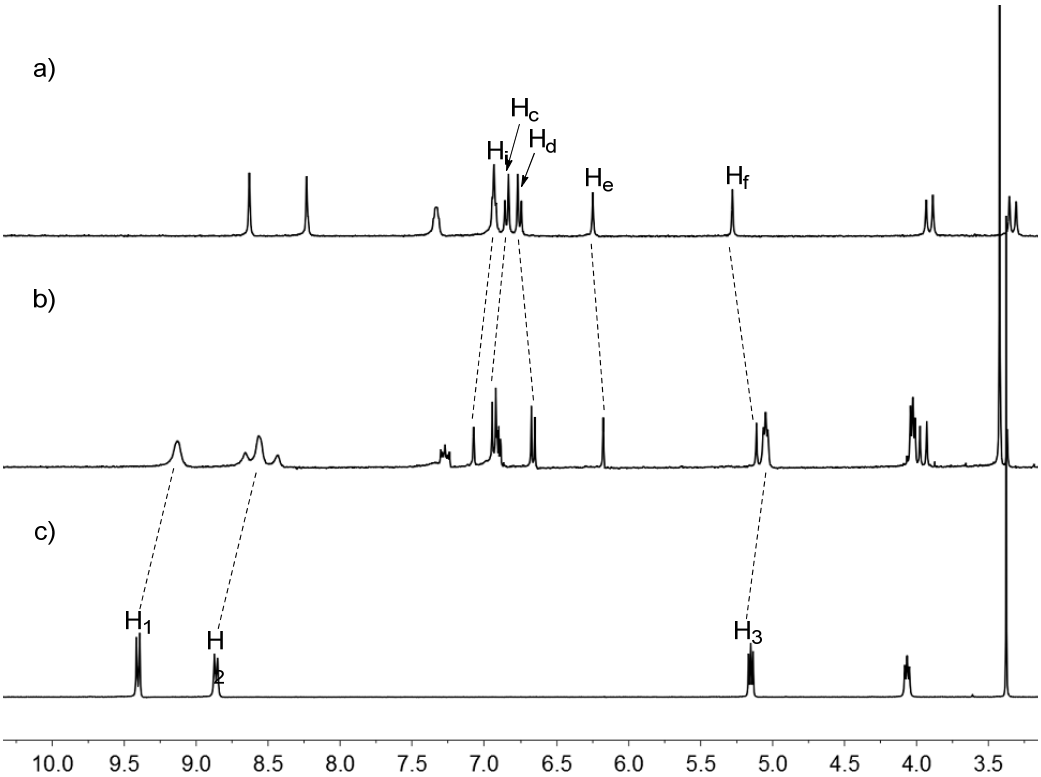

Fig. S42 Partial ^{1}H NMR spectra (300 MHz, acetone-d_6, 298 K) of (a) free host **11a**, (b) host **11a** with 1.0 equiv of **G4** and (c) free guest **G4**. [**11a**]$_0$ = 2.0 mM.

5. Determination of the mole ratio between host 11a and the guests

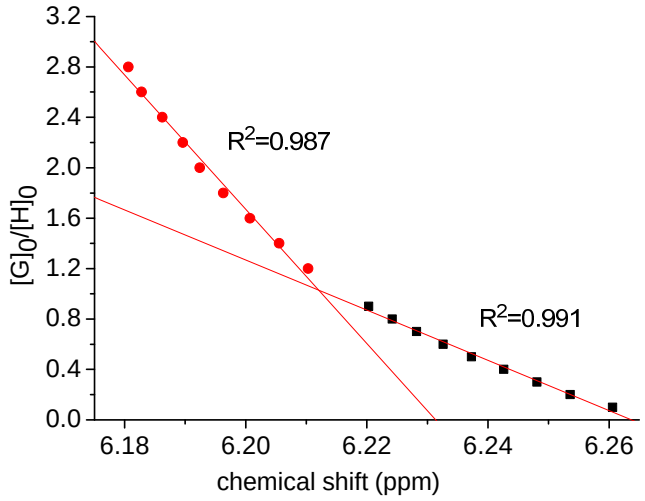

Fig. S43 Mole ratio plot for the complexation of **11a** and **G1** in acetone-d_6 at 298K.

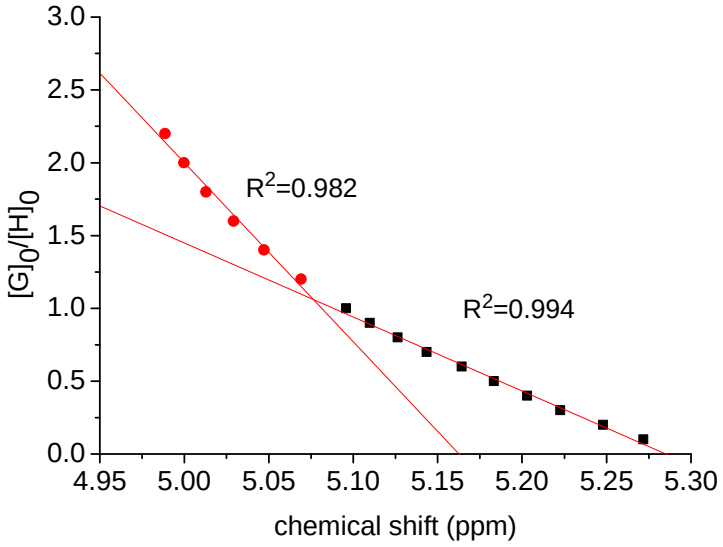

Fig. S44 Mole ratio plot for the complexation of **11a** and **G2** in acetone-d_6 at 298K.

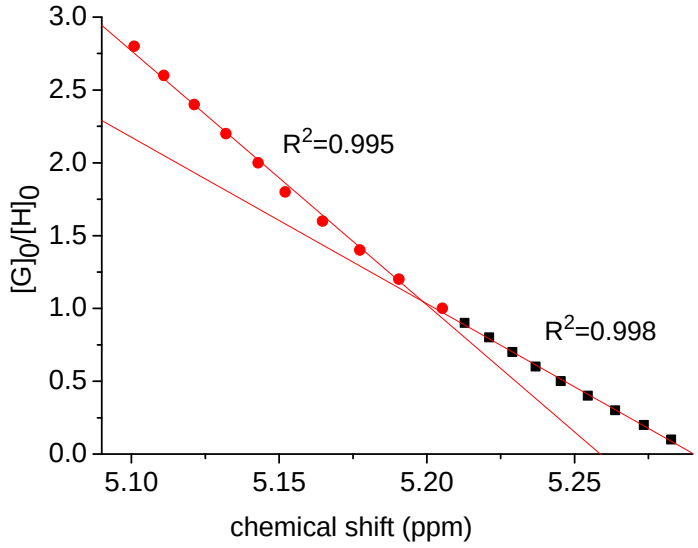

Fig. S45 Mole ratio plot for the complexation of **11a** and **G3** in acetone-d_6 at 298K.

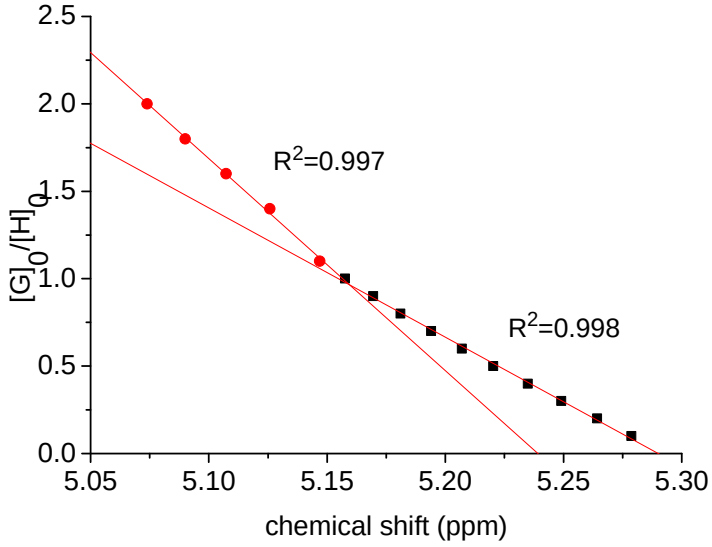

Fig. S46 Mole ratio plot for the complexation of **11a** and **G4** in acetone-d_6 at 298K.

6. ESI-MS spectra of the complexes

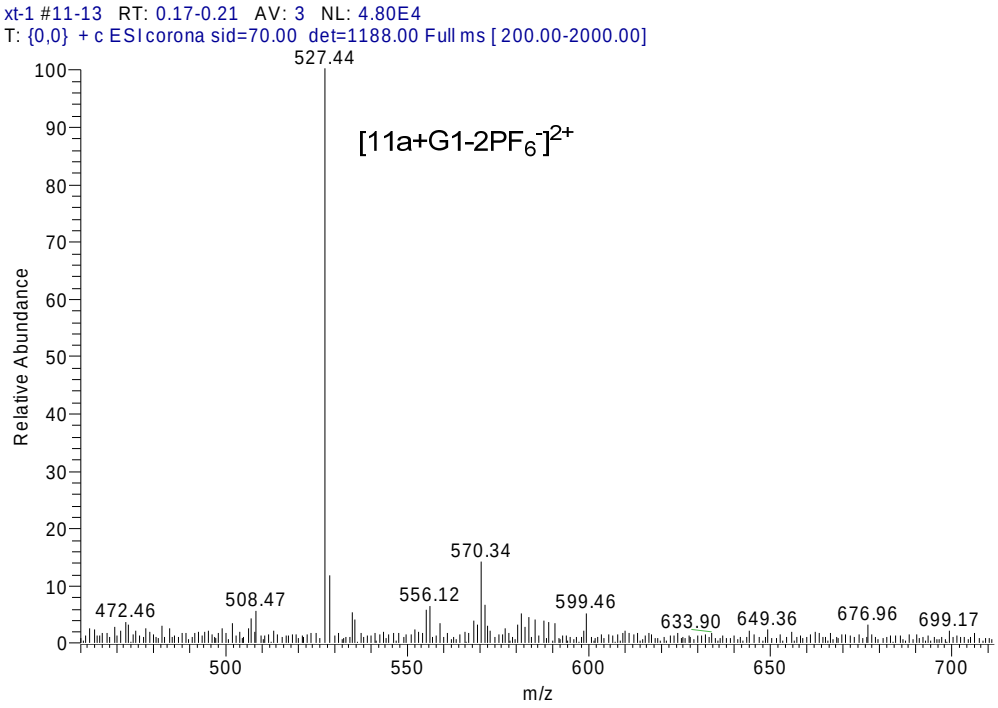

Fig. S47 ESI-MS spectrum of complex **11a·G1**.

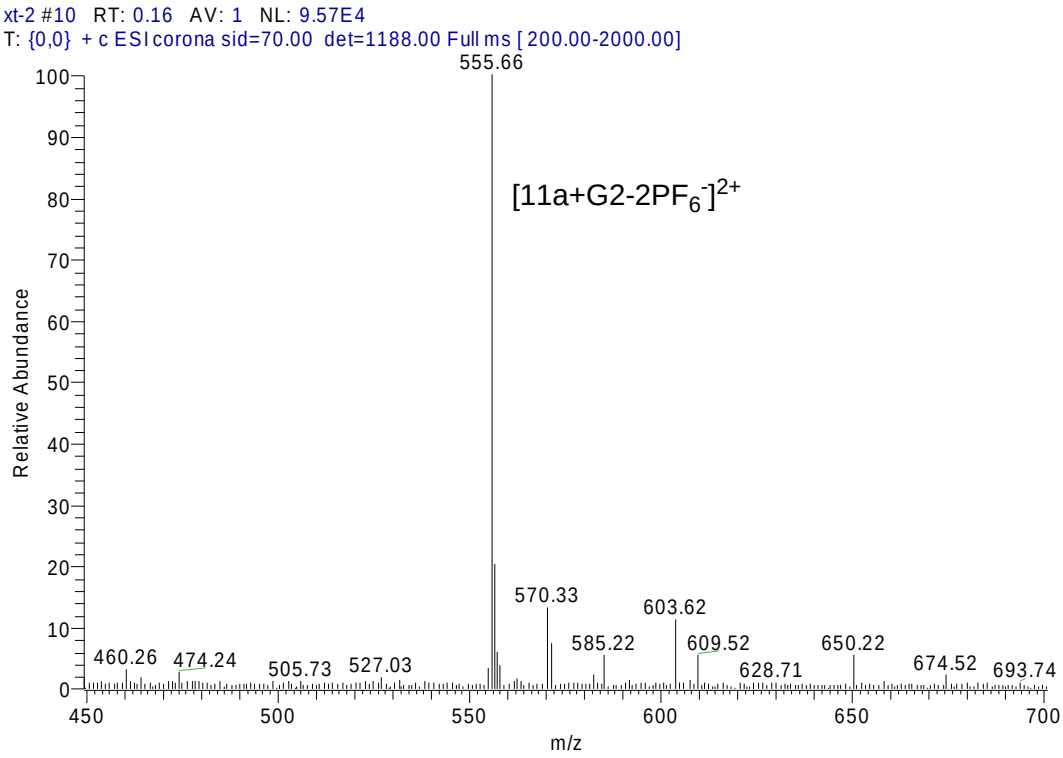

Fig. S48 ESI-MS spectrum of complex **11a·G2**.

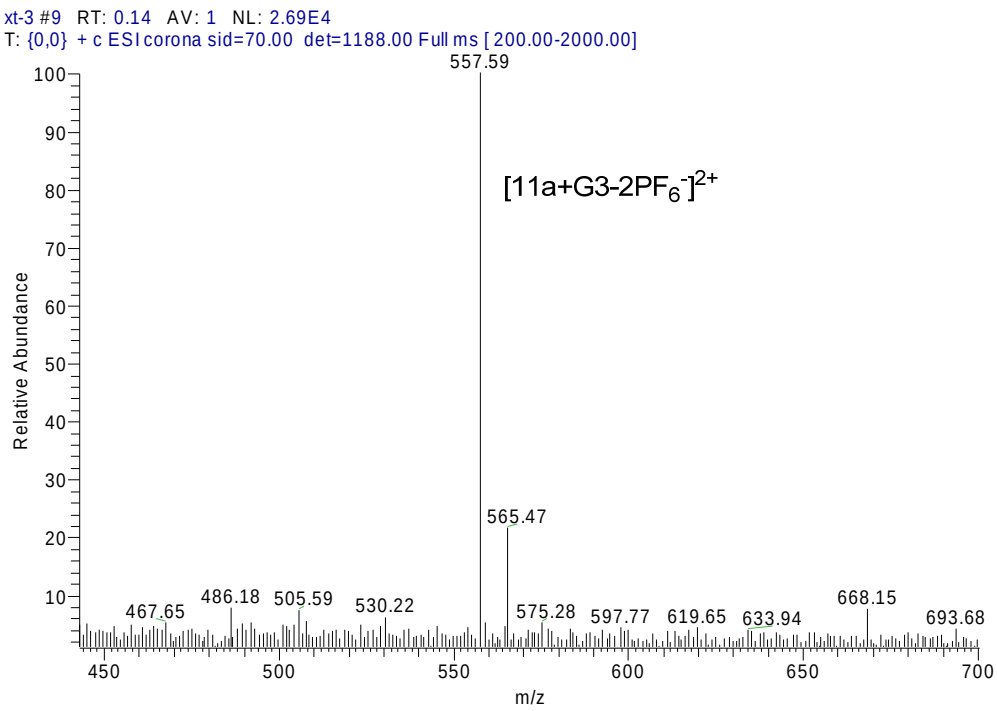

Fig. S49 ESI-MS spectrum of complex **11a·G3**.

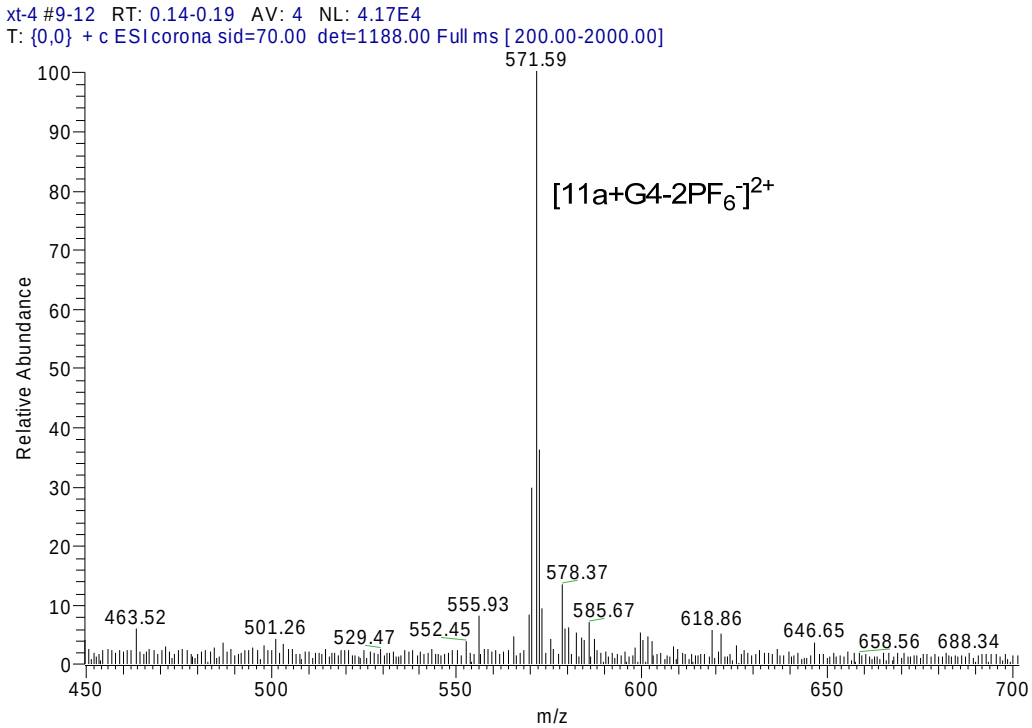

Fig. S50 ESI-MS spectrum of complex **11a·G4**.

7. ESI-HRMS spectrum of [2]rotaxane 15

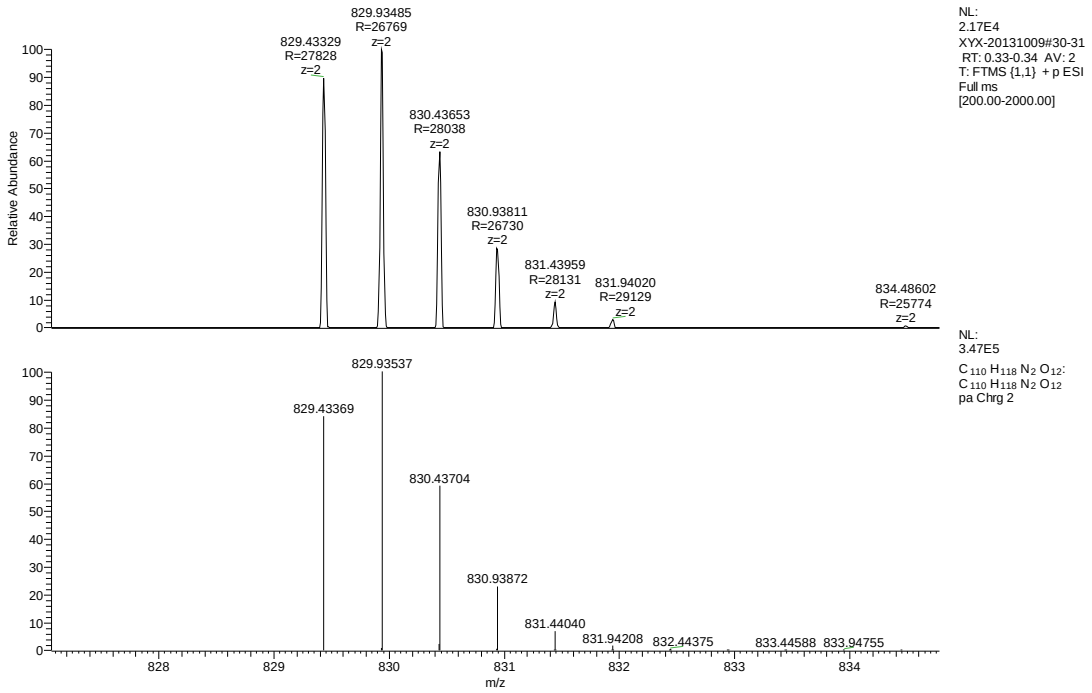

Fig. S51 ESI-HRMS spectrum of [2]rotaxane **15**.